NAVAL POSTGRADUATE SCHOOL

MONTEREY, CALIFORNIA

THESIS

SIMULINK-BASED IMPLEMENTATION AND PERFORMANCE ANALYSIS OF TDS-OFDM IN TIME-VARYING ENVIRONMENTS

by

Hui-Chen Lai

September 2014

Thesis Advisor: Monique P. Fargues
Co-Advisor: Roberto Cristi

Approved for public release;distribution is unlimited

THIS PAGE INTENTIONALLY LEFT BLANK

REPORT DOCUMENTATION PAGE

Form Approved OMB No. 0704–0188

1. AGENCY USE ONLY *(Leave blank)*	**2. REPORT DATE** September 2014	**3. REPORT TYPE AND DATES COVERED** Master's Thesis

4. TITLE AND SUBTITLE
SIMULINK-BASED IMPLEMENTATION AND PERFORMANCE ANALYSIS OF TDS-OFDM IN TIME-VARYING ENVIRONMENTS

5. FUNDING NUMBERS

6. AUTHOR(S) Hui-Chen Lai

7. PERFORMING ORGANIZATION NAME(S) AND ADDRESS(ES)
Naval Postgraduate School
Monterey, CA 93943-5000

8. PERFORMING ORGANIZATION REPORT NUMBER

9. SPONSORING /MONITORING AGENCY NAME(S) AND ADDRESS(ES)
N/A

10. SPONSORING/MONITORING AGENCY REPORT NUMBER

11. SUPPLEMENTARY NOTES The views expressed in this thesis are those of the author and do not reflect the official policy or position of the Department of Defense or the U.S. Government. IRB protocol number ____N/A____.

12a. DISTRIBUTION / AVAILABILITY STATEMENT
Approved for public release;distribution is unlimited

12b. DISTRIBUTION CODE
A

13. ABSTRACT (maximum 200words)

In this thesis, we develop simulink-based software models to implement and test the time-domain synchronous OFDM (TDS-OFDM) transmitter and receiver systems. This technique has been introduced in terrestrial digital broadcasting in the P.R.C., and it seems to be particularly suitable to highly mobile environments. The transmission channel is modeled as a time-varying Rayleigh multipath channel. Two standard transmission channels models are considered: the COST 207 model with 6-path typical urban (TU6) characteristics and the China test8 (CT8) model restricted to the 4-path characteristics only. Overall system performances are evaluated in terms of bit error ratio (BER) for different signal-to-noise ratio (SNR) levels in these two channel environments for mobile systems with various resulting Doppler shift levels. Results show the capabilities and limitations of this technology in estimating the time-varying transmission channel and reconstructing the transmitted data. Performances are also compared to those obtained by standard OFDM techniques, such as the one adopted by the digital video broadcasting terrestrial (DVB-T) standard.

14. SUBJECT TERMS Orthogonal Frequency-Division Multiplexing (OFDM), Time-Domain Synchronous OFDM (TDS-OFDM), Digital Terrestrial Multimedia Broadcasting (DTMB), Digital Terrestrial Television Broadcasting (DTTB), Digital Video Broadcasting- Terrestrial (DVB-T),communication system

15. NUMBER OF PAGES
91

16. PRICE CODE

17. SECURITY CLASSIFICATION OF REPORT	**18. SECURITY CLASSIFICATION OF THIS PAGE**	**19. SECURITY CLASSIFICATION OF ABSTRACT**	**20. LIMITATION OF ABSTRACT**
Unclassified	Unclassified	Unclassified	UU

NSN 7540–01-280-5500

Standard Form 298 (Rev. 2–89)
Prescribed by ANSI Std. 239–18

THIS PAGE INTENTIONALLY LEFT BLANK

Approved for public release;distribution is unlimited

SIMULINK-BASED IMPLEMENTATION AND PERFORMANCE ANALYSIS OF TDS-OFDM IN TIME-VARYING ENVIRONMENTS

Hui-Chen Lai
Lieutenant, Taiwanese Navy
B.S., R.O.C. Naval Academy, 2007

Submitted in partial fulfillment of the
requirements for the degree of

MASTER OF SCIENCE IN ELECTRICAL ENGINEERING

from the

NAVAL POSTGRADUATE SCHOOL
September 2014

Author: Hui-Chen Lai

Approved by: Monique P. Fargues
Thesis Advisor

Roberto Cristi
Co-Advisor

R. Clark Robertson
Chair, Department of Electrical and Computer Engineering

THIS PAGE INTENTIONALLY LEFT BLANK

ABSTRACT

In this thesis, we develop simulink-based software models to implement and test the time-domain synchronous OFDM (TDS-OFDM) transmitter and receiver systems. This technique has been introduced in terrestrial digital broadcasting in the P.R.C., and it seems to be particularly suitable to highly mobile environments. The transmission channel is modeled as a time-varying Rayleigh multipath channel. Two standard transmission channels models are considered: the COST 207 model with 6-path typical urban (TU6) characteristics and the China test8 (CT8) model restricted to the 4-path characteristics only. Overall system performances are evaluated in terms of bit error ratio (BER) for different signal-to-noise ratio (SNR) levels in these two channel environments for mobile systems with various resulting Doppler shift levels. Results show the capabilities and limitations of this technology in estimating the time-varying transmission channel and reconstructing the transmitted data. Performances are also compared to those obtained by standard OFDM techniques, such as the one adopted by the digital video broadcasting terrestrial (DVB-T) standard.

THIS PAGE INTENTIONALLY LEFT BLANK

TABLE OF CONTENTS

LIST OF FIGURES

LIST OF TABLES

THIS PAGE INTENTIONALLY LEFT BLANK

LIST OF ACRONYMS AND ABBREVIATIONS

ASK	amplitude-shift keying
ATSC	advanced television system committee
AWGN	additive white Gaussian noise
BER	bit error ratio
CFR	channel frequency response
CIR	channel impulse response
COFDM	coded orthogonal frequency-division multiplexing
CP	cyclic prefix
CT8	China Test 8
DAB	digital audio broadcast
DTMB	digital terrestrial multimedia broadcasting
DTTB	digital terrestrial television broadcasting
DTV	digital television
DVB-T	digital video broadcasting-terrestrial
FEC	forward error correction
FFT	fast Fourier transform
FSK	frequency-shift keying
FT	Fourier transform
GI	guard interval
HDTV	high-definition television
IFFT	inverse fast Fourier transform
ISDB-T	integrated services digital broadcasting-terrestrial
ISI	inter-symbol interference
LOS	line-of-sight
MCM	multicarrier modulation
NTSC	National Television Standards Committee
OFDM	orthogonal frequency-division multiplexing
OLA	overlap and add
PDF	probability density function
PN	pseudo noise

P.R.C.	People’s Republic of China
PSK	phase-shift keying
QAM	quadrature amplitude modulation
QPSK	quadrature phase-shift keying
SC	single carrier
SFN	single-frequency network
SNR	signal-to-noise ratio
S/P	serial-to-parallel
TDS-OFDM	time-domain synchronous OFDM
TPS	transmission parameter signaling
TU6	Typical Urban 6-path channel
ZP	zero prefix

EXECUTIVE SUMMARY

Wireless communication systems are more complex than the wired communication versions because of the inherent multipath propagation issues present within. In addition, the Doppler frequency shift due to the relative motion between transmitter and/or receiver makes it more challenging and degrades the system performance.

To fulfill the increasing demand for high throughput and data rate implementation for the communication system while mitigating the system degradation due to the fading factors in the wireless environment, orthogonal frequency-division multiplexing (OFDM) (a special case of multicarrier modulation technique that is known for combating the multipath and inter-symbol interference [ISI] by utilizing several orthogonal subcarriers) has been recently adopted as a standard in numerous wireless applications.

The purpose of this thesis is to evaluate the performance of the OFDM technique used in terrestrial broadcasting. In particular, our interest is in the newly proposed OFDM approach, time-domain synchronous OFDM (TDS-OFDM), currently adopted as the TV standard of the People's Republic of China and called DTMB.

First, a proposed wireless communication system for TDS-OFDM in Simulink is designed according to the specifications of the TV standard, DTMB. To account for the natural characteristics of the wireless communications environment, channels with multipath fading and Doppler shift need to be considered. Two standard channel models, the 6-path typical urban (TU6) channel in COST 207 and the modified 4-path China Test 8 (CT8), were employed in our model to simulate the multipath channel with Rayleigh fading characteristics.

In the proposed Simulink model, the multicarrier modulation version of OFDM is utilized for the modulation and demodulation processes. To recover the transmitted signal for bit error ratio (BER) evaluation in the presence of a time-varying scenario, channel estimation and tracking is conducted in the frequency domain by a fast Fourier transform (FFT) operation. The estimated channel impulse response is then fed into equalization to recover the transmitted signal.

To validate the effectiveness of the proposed system, the performance of the TDS-OFDM system is first tested for a frequency-selective, slow-fading channel. In addition, the Simulink model for DVB-T, the corresponding counterpart of DTMB that employs the conventional cyclic prefix-OFDM (CP-OFDM), is also presented and the comparison between DTMB and DVB-T are conducted.

The system performance in this thesis is evaluated on the basis of BER for different signal-to-noise ratio (SNR) levels. The experimental results of TDS-OFDM obtained over both TU6 and modified CT8 channels are similar. Simulation results show the proposed TDS-OFDM system has low BER for high SNR or low Doppler shift in both TU6 and modified CT8 channel environments. Performance over non-multipath and time-invariant channel environments is also evaluated as a reference for performance degradation comparison. As expected, in terms of BER, TDS-OFDM shows an improvement with respect to the standard CP-OFDM in cases of high mobility and high SNR level.

The results obtained for DTMB and DVB-T show that DTMB outperforms DVB-T for high SNR, generally above 20 dB depending on the specific channel environment, for all corresponding Doppler shift cases considered for both channel models. These results also confirm that TDS-OFDM is faster than the classic CP-OFDM in adapting to changes in the physical time-varying channel, as reflected by lower BER for DTMB in highly mobile environments. Without the addition of forward error correction coding and interleaving in the proposed system, the BER improvement is limited, especially in the fast time-varying environment. Note that the results obtained in this research are not limited to terrestrial broadcasting but are applicable to any general mobile wireless communication system.

ACKNOWLEDGMENTS

The completion of this thesis does not mean the end of the journey for exploring knowledge. I am very grateful to have had the chance to pursue the master's degree at Naval Postgraduate School. Without the support and encouragement from my dear parents, friends, and classmates, as well as professors, I could not have accomplished this goal.

First of all, I would like to recognize the Taiwanese Navy and Chung Cheng Institute of Technology National Defense University for giving me the opportunity to pursue a master's degree in this well-known graduate school.

I would also like to express my gratitude to my advisor, Professor Monique P. Fargues, for her patience and valuable guidance that always gave me so much confidence whenever I was lost.

To Professor Roberto Cristi, I am very appreciative of his patience for guiding me not only on my thesis but also throughout my studies in the ECE Department.

I am really thankful for the encouraging atmosphere both professors created during this research journey, which made it a very enjoyable experience.

Finally, I would like to dedicate this work to my parents, who are not only being supportive and patient as they always have been, but also for constantly providing me with inspiration and courage for achieving my goals.

THIS PAGE INTENTIONALLY LEFT BLANK

I. INTRODUCTION

High data rate communication systems are an integral part of life today, especially in defense applications. The necessity of transferring a high volume of data in real time is critical to the success of missions involving mobile units.

One of the most successful digital modulation techniques is orthogonal frequency-division multiplexing (OFDM), which is capable of transferring large blocks of data at a time even in the presence of poorly known wireless channels. By contrast, standard single-carrier modulation requires complex and unreliable channel equalization, which is not the case for OFDM.

The area of digital broadcasting has fueled quite a bit of research in high data rate communications, especially due to the commercialization of high-definition television for mobile devices. It turns out that in most of the world OFDM is at the basis of standards for digital TV and audio broadcasting.

A. OFDM FOR WIRELESS COMMUNICATIONS AND DIGITAL BROADCASTING

Digital terrestrial television broadcasting (DTTB) currently attracts a significant amount of attention in television services, as it provides for faster and more reliable transmission than conventional analog television services do. In addition, reliable wireless communication techniques must be applied to handle increasing demands for high data rate and the capacity needed for terrestrial television communication schemes. Moreover, the wireless transmission medium for terrestrial television communication is challenging due to multipath propagation and mobility issues that must be taken into account. To overcome the inherent channel impairments in wireless environments, a number of terrestrial communication systems and standards have been developed, and some approaches have been proposed in several studies. OFDM is one of the most popular digital modulation techniques and has been adopted as the standard for numerous wireless applications, such as digital video and audio broadcast (DVB and DAB,

respectively), asymmetric digital subscriber line (ADSL), and wireless LAN standards, including 802.11a and 802.11g.

The conventional implementation of OFDM is based on what is called cyclic prefix-OFDM (CP-OFDM), which is common in all of the aforementioned communication applications. With this approach, the time-varying wireless channel is tracked by properly placed "pilot" subcarriers, whose content is known at the receiver.

Since an accurate OFDM demodulation process relies on a good estimate of the wireless channel, mobile applications in high-speed vehicles call for fast channel acquisition and tracking. Improvements at the demodulation stage were recently obtained with an OFDM variant, which is based on a newly proposed time-division synchronization OFDM (TDS-OFDM) scheme. At the present time this approach is mainly implemented in digital terrestrial multimedia broadcasting (DTMB) systems as the standard for digital television service in the People's Republic of China (P.R.C.) and is not yet officially adopted for other communication applications. The goal of this study is to investigate whether TDS-OFDM may be considered as a viable option for mobile wireless communication since results obtained in this research are not limited to digital broadcasting applications only.

Some OFDM schemes use pilots located in the data frame to track changes in the channel characteristics, as reported in [1], [2], [3], and [4]. These pilot-based methods, however, have a lower spectral efficiency than those based on using the pseudo noise (PN) sequence located in the frame prefix. Typically, these latter techniques are classified into one of two categories: those based on time-domain or frequency-domain channel estimation schemes. In most literature, the time-domain channel estimation approach is based on using the correlation between the received signal and the PN sequence as in [5], [6], [7], [8], and [9].

The objective of this thesis is to evaluate and analyze the performance of the TDS-OFDM-based DTTB standard, DTMB, in a time-varying multipath communication channel by utilizing a frequency-domain-based channel estimation and equalization approach. OFDM system performance is evaluated in terms of bit error ratio (BER) for

different SNR levels. Physical phenomena encountered when dealing with wireless applications such as multipath fading and Doppler shift issues are taken into consideration in the simulations. Two channel models, COST 207 Typical Urban (TU6) and modified China Test 8 (CT8), with different terrain and power delay profiles are considered in the study to model the multipath channel. Simulations are conducted using Simulink.

B. THESIS ORKGANIZATION

The thesis is organized as follows. Chapter II starts with a discussion of the general wireless communication environment and the different types of fading that may occur in the wireless scenario are described. Next, basic concepts used in OFDM techniques are introduced, and two types of OFDM-based DTTB standards—DTMB and DVB-T—are presented in Chapter III. The two channel models considered in the study and specifics regarding transmitter and receiver systems used in TDS-OFDM are described in Chapter IV. Simulation results are presented in Chapter V. Finally, conclusions and recommendations for future work are presented in Chapter VI.

THIS PAGE INTENTIONALLY LEFT BLANK

II. BACKGROUND

It is well known that wireless communication channels are more unpredictable than their wired counterparts due to fading factors present in the wireless communication environment. The undesired fading loss in terrestrial applications is usually caused by multipath propagation and Doppler frequency shift. These two factors also further affect the system performance in terrestrial communication [10].

The issues introduced by the presence of multipath and Doppler shift in wireless communication systems are first discussed in this chapter. Then, existing digital terrestrial television standards are introduced. Finally, the modulation techniques employed in this thesis are described briefly.

A. MOBILE-RADIO PROPAGATION CHARACTERIZATION

Thermal noise generated in a receiver is usually the primary noise responsible for system degradation in digital communication systems. The ideal thermal noise model used in the analysis of communication systems is additive white Gaussian noise (AWGN), which is known for its flat power spectral density in the frequency domain. In practical wireless mobile applications, however, a signal that propagates from transmitter to receiver does so through different paths due to reflection, diffraction, and scattering in the environment. In addition, the relative mobility of a transmitter and/or receiver creates a Doppler shift effect in the received signal; therefore, noise and fading factors cause signal fluctuations that make terrestrial communication channels selective in time and frequency [10].

1. Fading Factors in Wireless Communication Channels

a. Multipath

Multipath delay results from a transmitted signal reflected by objects such as hills, buildings, and cars in the propagation path. A reflected signal may go through different paths to reach a receiver, and the signal's power also suffers from different degrees of

attenuation depending on constructive or destructive superposition of the delayed copies of the signal [11]. The illustration of multipath propagation is shown in Figure 1.

Time dispersion due to multipath propagation causes further inter-symbol interference (ISI) [10], where the energy of a transmitted signal symbol extends into the next one, introducing distortion in the received signal. Additionally, the channel frequency response (CFR) magnitude is not reliably constant within the signal bandwidth B_s when the channel time spread from multipath propagation is longer than the symbol duration. In addition, mobility also causes frequency-selective fading, which is defined to be when the coherence bandwidth of the channel B_c is smaller than that of the transmitted signal B_s [11]. The concept of frequency-selective fading is discussed in detail later.

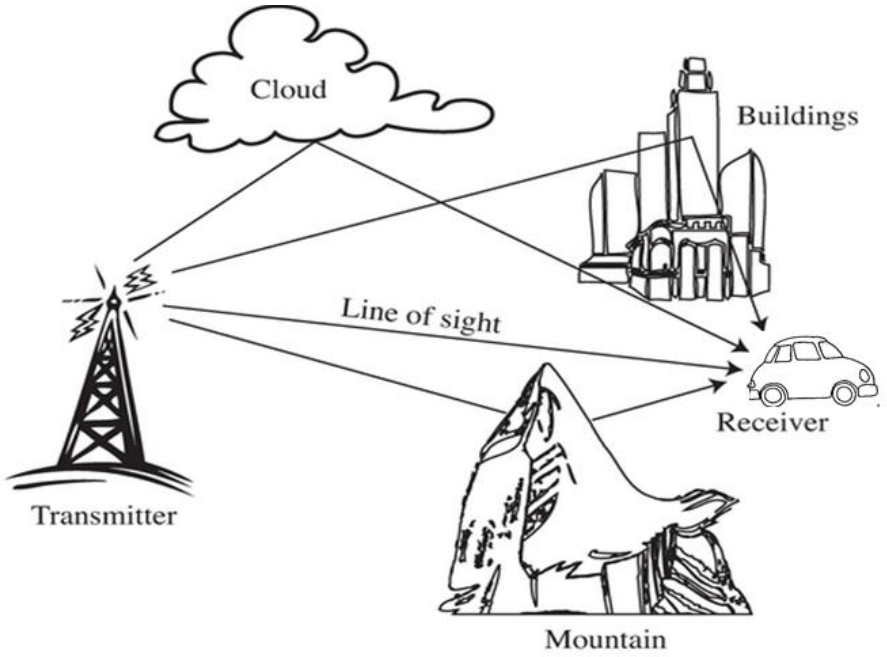

Figure 1. Illustration of multipath propagation effects where the received signal is the combination of several copies of transmitted signal with different delays and attenuations (after [13]).

b. Doppler Effect

In mobile communication environments, the relative motion between transmitter and receiver also causes a Doppler frequency shift in the received signal [12]. Doppler shift is also sometimes called frequency dispersion because the transmitted signal is shifted and spread in the frequency domain. An illustration of Doppler spread is shown in Figure 2, and the general Doppler shift can be expressed as

$$f_D = \frac{v}{c} f_c \cos\alpha , \tag{2.1}$$

where f_c is the carrier frequency in Hz, v is the relative velocity between transmitter and receiver in m/s, α is the angle between the direction of the transmitter and the wave motion, and c is the speed of light in terrestrial communication (3×10^8 m/s). The maximum Doppler shift is then given as

$$f_{D\max} = \frac{v}{c} f_c \ . \tag{2.2}$$

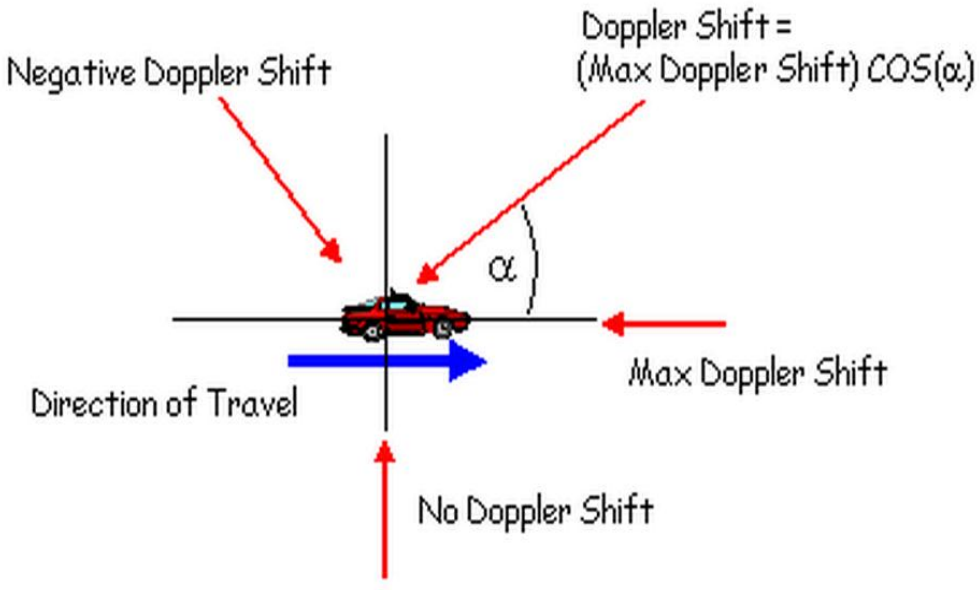

Figure 2. Details of Doppler spread (from [5]).

2. Types of Fading

a. Coherence Time and Coherence Bandwidth

Fading occurs when the strength of a received signal varies with time. Due to the combination of multipath propagation and the relative motion between transmitter and receiver, fading causes time-varying attenuation as well as delays that may significantly degrade communication system performance. Multipath propagation in combination with the Doppler effect causes frequency- and time-selective fading. [12]

The specific type of fading channel usually depends on the physical channel characteristics, namely channel coherence time T_c and channel coherence bandwidth B_c. The channel coherence time T_c depends on the Doppler shift, while the channel coherence bandwidth B_c is affected by the amount of time delay due to the multipath present in the channel.

To evaluate the impacts multipath propagation and Doppler shift have on the performance of communication systems, the fading mechanism that may be present in wireless channels must first be understood. Selectivity and dispersion are time-frequency dual mechanisms of the fading channel where the dispersion in time due to the multipath propagation causes selectivity in frequency, while the dispersion in frequency due to the Doppler shift causes selectivity in time.

Frequency selectivity is defined by the coherence bandwidth, which represents the approximate bandwidth where the magnitude of the CFR is assumed to be nearly constant. The coherence bandwidth can be described as

$$B_c \approx \frac{1}{5\tau_{\max}}, \tag{2.3}$$

where $\tau_{\max}$ is defined as the maximum channel time spread [10]. The coherence time T_c refers to the approximate time duration during which the CFR magnitude is assumed to be nearly constant. The coherence time can be described as

$$T_c = \frac{9}{16\pi f_{D\max}} \text{ (according to the 50\% correlation rule)}, \tag{2.4}$$

where $f_{D\max}$ represents the maximum Doppler shift value [10].

b. Fading Channel Classification:

Coherence bandwidth B_c and coherence time T_c are parameters used to describe the behavior of the transmission channel in both the time and frequency domains. Four different types of fading can be defined depending on specific values for coherence bandwidth and time, signal bandwidth B_s and signal duration T_s, as illustrated in Figure 3.

(1) Fading due to multipath: A transmission channel is classified as a frequency-non-selective channel or a flat-fading channel when the CFR can be assumed to be constant within the bandwidth B_c when $B_s < B_c$ $(\tau_{\max} < T_s)$.

(2) Fading due to multipath: A transmission channel is referred to as a frequency-selective channel when $B_s > B_c$ where the CFR magnitude has variations within B_s.

(3) Fading due to Doppler shift: If $T_c > T_s$ (low $f_{D\max}$), a transmission channel is classified as a slow-fading channel where the CFR can be assumed to be constant for times as long as T_c.

(4) Fading due to Doppler shift: When $T_c < T_s$, the channel is referred to as fast fading where the CFR does not remain constant for times as long as T_s.

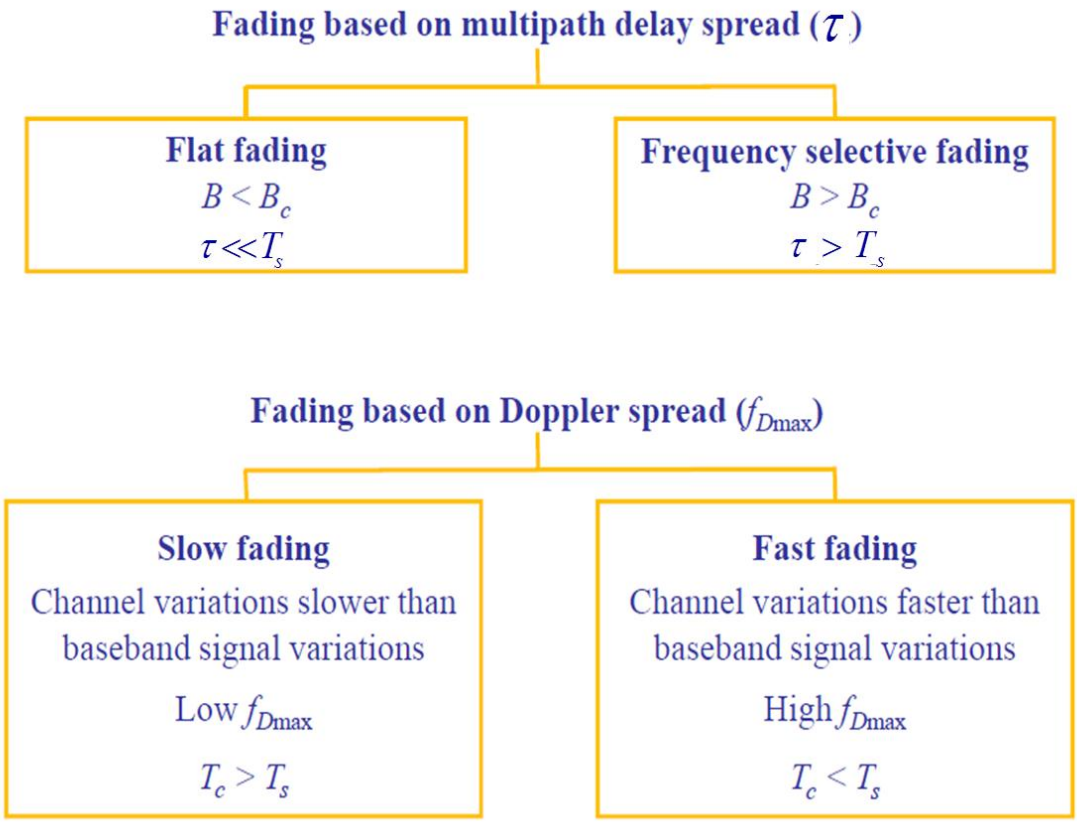

Figure 3. Various types of fading based on B_c and T_c (from [15]).

The four types of fading (flat fading, frequency-selective fading, slow fading, and fast fading) yield four possible types of physical channels associated with specific factors, as shown in Figure 4.

In terrestrial mobile communication, the flat-fading channel and slow-fading channel are desired channel models when fading issues are under consideration. The channel, however, is often both frequency-selective and fast fading due to higher channel time spread and the relative motion between transmitter and receiver in mobile wireless applications; therefore, it is best if those factors can be taken into account in system design and performance evaluation phases.

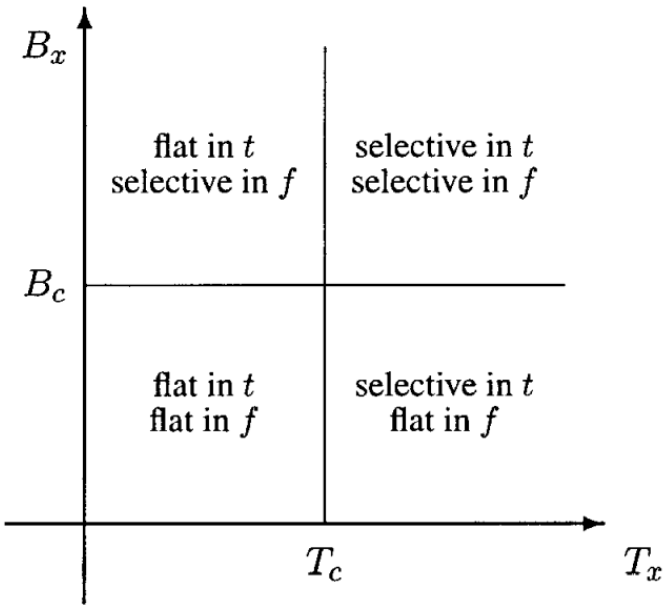

Figure 4. Radio-channel classification (from [12]).

3. Statistical Model of Multipath Fading Channel

Fading is a random phenomenon described by a statistical model according to the specific type of environment. When a dominant signal component, often called a line-of-sight (LOS) component, exists, the envelope of the channel response is often modeled as having a Rician probability density function (pdf), which is given by

$$f_R(r) = \frac{r}{\sigma^2}\exp\left(-\frac{(r^2+K^2)}{2\sigma^2}\right)\mathrm{I}_0\left(\frac{Kr}{\sigma^2}\right),\ r \geq 0,\ K \geq 0, \tag{2.5}$$

where r is the absolute value of the amplitude, σ^2 is the signal power, $I_0(.)$ is the modified Bessel function of order zero, and factor K is defined as $K = P_{LOS}/P_{NLOS}$, where P_{LOS} is the LOS signal power; and P_{NLOS} is the NLOS signal power [15]. The Rician pdf with different values of the factor K is shown in Figure 5. Note that if $K \to \infty$, the channel is said to have additive white Gaussian noise (AWGN). When no LOS exists, which typically occurs in outdoor environments, $K = 0$, and the channel response envelope is modeled with a Rayleigh pdf, which is a special case of the Rician pdf.

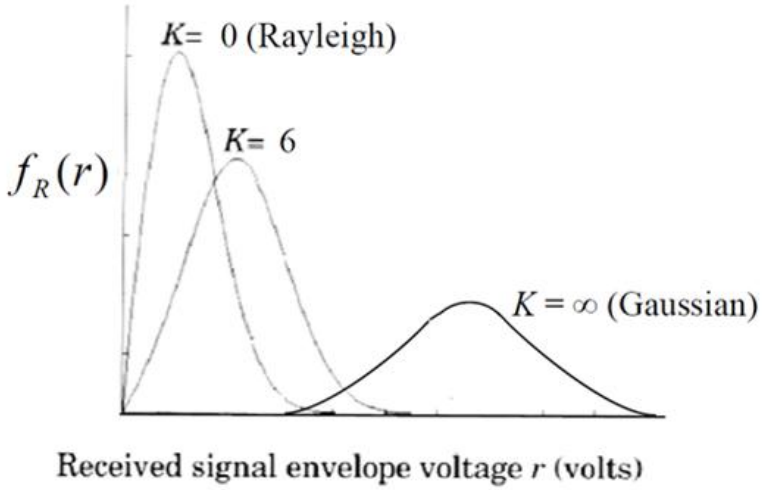

Figure 5. A family of Rician probability density functions, parameterized by the variable K (from [15]).

Rayleigh fading is used to simulate the fluctuations in the amplitude of the received signals due to multipath fading channel when there is no LOS signal component present. It is often classified as the worst type of fading. The Rayleigh pdf is given as

$$f_R(r) = \frac{r}{\sigma^2} \exp\left(-\frac{r^2}{2\sigma^2} \right), \; r \geq 0 . \tag{2.6}$$

Several examples of the Rayleigh probability density function obtained with different standard deviation values are shown in Figure 6.

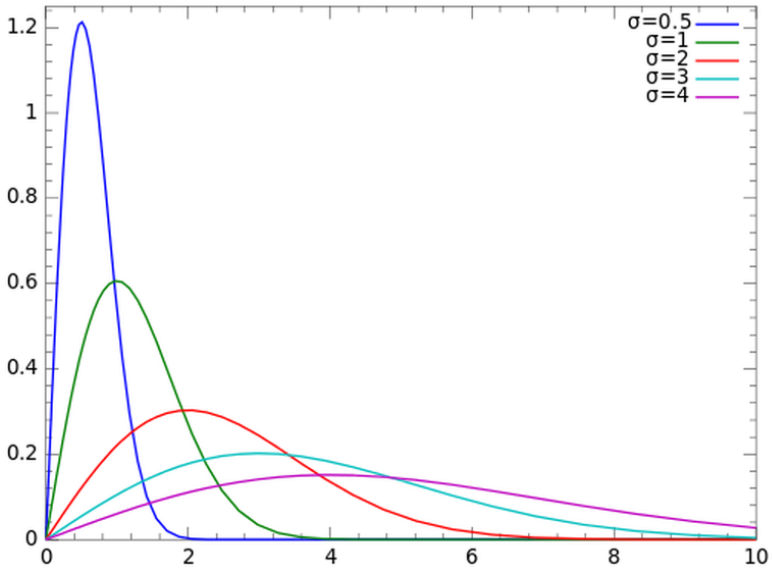

Figure 6. Rayleigh probability density function with different standard deviation values (from [8]).

B. DIGITAL TERRESTRIAL TELEVISION

Due to the increasing demand for bandwidth-efficient and high-throughput multimedia services in television broadcasting applications, the evolution from analog to digital is an important trend in new terrestrial communication standards. Digital television (DTV) services can be delivered via terrestrial, satellite, cable and so on. Among those, digital terrestrial television broadcasting (DTTB) is the most attractive scheme among DTV services.

DTV and conventional analog terrestrial television signals propagate in the same fashion. The main feature of DTV is multiplexing transmission, which allows for the use of multiple sub-channels in single-frequency networks (SFN). Compared to analog terrestrial transmission, DTV also provides less interference, better video quality, better spectral efficiency, and more services such as mobile reception or high-definition television (HDTV). Overall, DTV outperforms analog terrestrial television and has become the dominant terrestrial communication technique nowadays [17].

1. Existing TV Standards

Four major DTTB standards for TV signals transmitted in the VHF and UHF frequency bands exist nowadays; their geographical usages are shown in Figure 7.

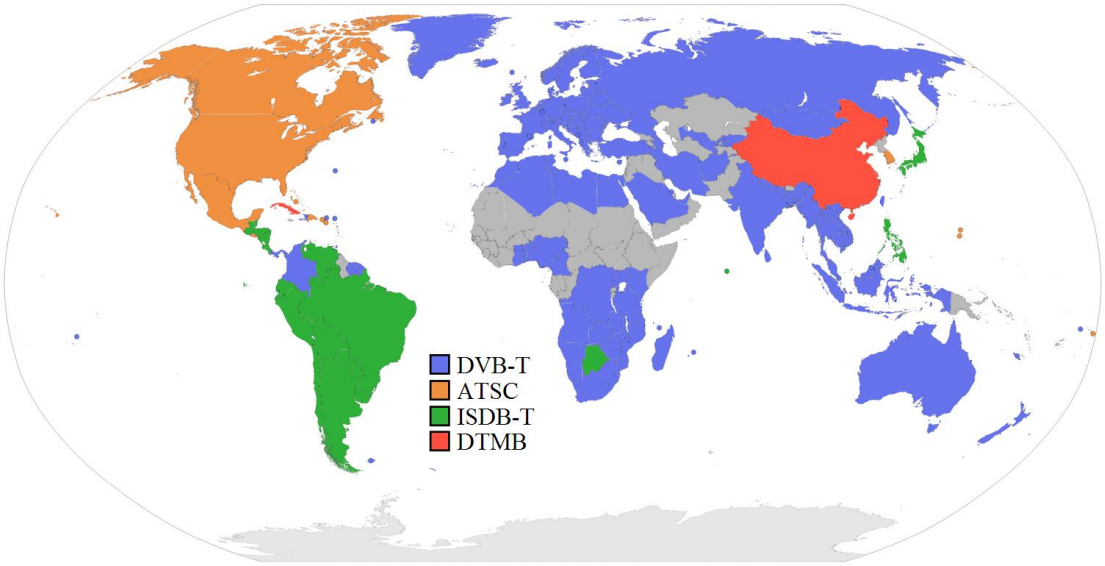

Figure 7. Geographical usages of TV broadcasting standards (from [18]).

Advanced Television System Committee (ATSC) is used mainly in North America. This standard is an evolution from conventional analog National Television Standards Committee (NTSC), with eight-level amplitude-shift keying (8-ASK) modulation; ATSC is more resistant to interference distortions than digital video broadcasting-terrestrial (DVB-T) but is less resistant to multipath distortion.

Digital Video Broadcasting-Terrestrial (DVB-T) is used mainly in Europe and also has been adopted in Russia, Australia, India, North African countries, the Middle East, Taiwan, and many other countries. This standard is based on standard OFDM with either 16- or 64-quadrature amplitude modulation (QAM). In theory, a channel with higher-level modulation is capable of transmitting with a higher bit-rate but needs more power to obtain the specific BER performance and is more susceptible to interference distortions.

Integrated Services Digital Broadcasting-Terrestrial (ISDB-T) is used mainly in Japan. This standard is based on standard OFDM and is similar to DVB-T.

Digital Terrestrial Multimedia Broadcasting (DTMB) is used mainly in China. This standard is based on time-domain synchronous OFDM (TDS-OFDM), where the level of the M-QAM modulation can either be 4, 16, 32, or 64. DTMB proponents claim this standard has faster and more accurate channel tracking than the DVB-T standard does due to its use of TDS-OFDM.

Please refer to [19], [20], and [21] for further details on these international standards. All standards except ATSC use OFDM modulation technology with different OFDM symbol structures—which is discussed later in detail—while ATSC uses ASK modulation.

C. MODULATION SCHEME-QAM

In digital communications, the amount of data transmitted depends on the channel capacity and the channel modulation scheme. Communication systems are often required to achieve both high spectral efficiency and throughput.

The modulation scheme used in OFDM-based DTTB standards is OFDM with M-level quadrature amplitude modulation (M-QAM).

QAM is a digital modulation scheme that conveys data by modulating the amplitudes of two out-of-phase carrier waves (usually sinusoid waves). Compared to M-ary phase-shift keying (MPSK) with constant amplitude, the signal symbols in QAM have different amplitudes and phases. In other words, QAM can be seen as quadrature amplitude-shift keying (ASK). Since digital communication data are binary, M-QAM utilizes $M = 2^k$ where k is an integer to represent M distinct symbols with finite energy and non-constant amplitude. The transmitted signal generated for M-QAM is given as

$$s_i(t) = \sqrt{\frac{2E_{min}}{T_s}} a_i \cos(2\pi f_c t) + \sqrt{\frac{2E_{\min}}{T_s}} b_i \sin(2\pi f_c t),\ 0 \le t \le T_s,\ i = 1, 2, \ldots, M, \quad (2.7)$$

where E_{min} is the minimum energy of the signal, and a_i, b_i are pairs of independent integers selected according to the location of the particular signal point. The $\sqrt{M} \times \sqrt{M}$

array of pairs (a_i, b_i) observed for an M-QAM constellation, where $M = 16$, can be defined as

$$\{a_i, b_i\} = \begin{bmatrix} (-3,3) & (-1,3) & (1,3) & (3,3) \\ (-3,1) & (-1,1) & (1,1) & (3,1) \\ (-3,-1) & (-1,-1) & (1,-1) & (3,-1) \\ (-3,-3) & (-1,-3) & (1,-3) & (3,-3) \end{bmatrix}. \tag{2.8}$$

The M-QAM signal set defined over $0 \le t \le T_s,$ for $i = 1, 2, \ldots, M$ in (2.7) can be rewritten as

$$s_i(t) = \sqrt{E_{min}} a_i \phi_I(t) + \sqrt{E_{min}} b_i \phi_Q(t) \tag{2.9}$$

by defining the two orthogonal functions ϕ_I and ϕ_Q as

$$\begin{aligned} \phi_I(t) &= \sqrt{\frac{2}{T_s}} \cos(2\pi f_c t); \\ \phi_Q(t) &= \sqrt{\frac{2}{T_s}} \sin(2\pi f_c t); \end{aligned} \quad .[15] \tag{2.10}$$

Note that more bits can be transmitted within a symbol with higher-order constellation configurations. The resulting symbols, however, are closer and more susceptible to noise as the constellation configuration order increases, resulting in higher BERs. Therefore, higher SNR levels are required when using higher-order QAM schemes to ensure a given BER. In DTMB, constellation levels (M) are often selected as 4, 16, 32, and 64. For the simulations conducted in this thesis, we selected $M = 16$ for QAM. The resulting rectangular constellation diagram obtained for the 16-QAM configuration is shown in Figure 8.

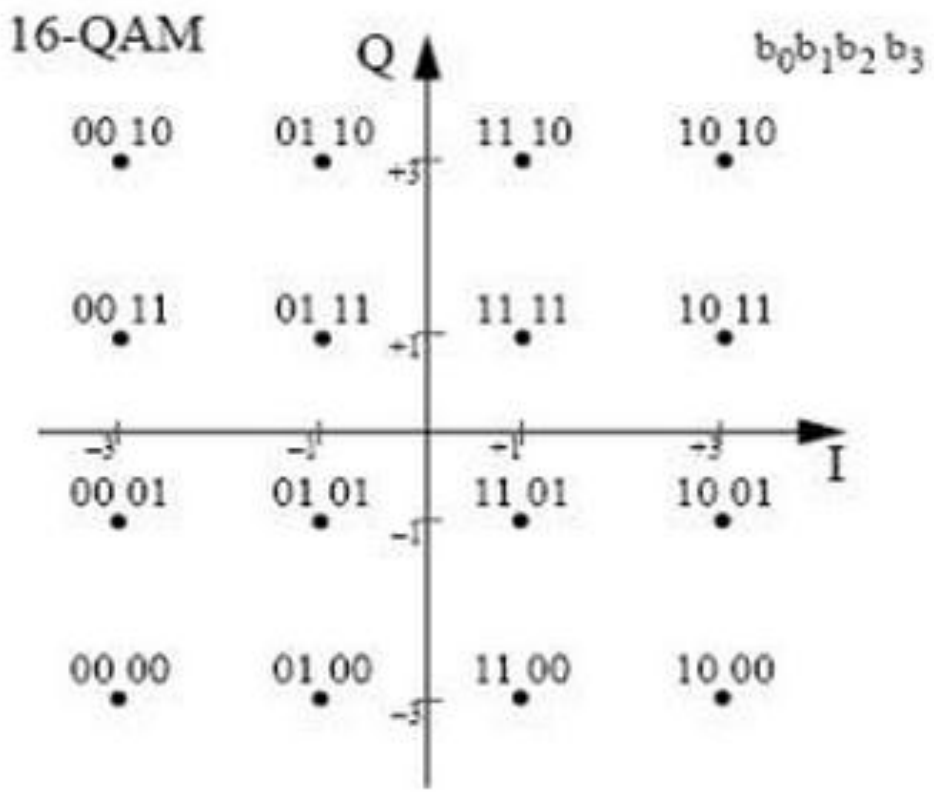

Figure 8. Signal constellation of 16-QAM (from [22]).

Digital modulation is at the basis of multi-carrier modulation and OFDM is described in the next chapter.

THIS PAGE INTENTIONALLY LEFT BLANK

III. OFDM TECHNIQUE FUNDAMENTALS

The general concept of OFDM is introduced in this chapter. First, the guard interval (GI) of OFDM is introduced, followed by a description of the number of OFDM classes that can be defined according to the specified GI. Finally, two types of OFDM-based digital terrestrial television broadcasting transmission standards, DTMB and DVB-T, are discussed.

A. ORTHOGONAL FREQUENCY-DIVISION MULTIPLEXING (OFDM)

Orthogonal frequency-division multiplexing is a particular case of multi-carrier modulation (MCM). The idea behind MCM is that instead of transmitting data symbols at high rate (R) using only one carrier, blocks of N data symbols are transmitted in parallel using N subcarriers, each one at a lower rate (R/N). As a result, the symbol length of each subcarrier ($T_{sb} = NT_s$) can be increased to be much larger than the channel delay spread (τ), thus combatting ISI. Furthermore, by imposing certain orthogonality conditions and choosing a sufficiently large number of subcarriers, a particular class of MCM can be defined (referred to as OFDM) where every subcarrier sees a flat-fading channel, even in the presence of an overall frequency-selective channel.

In OFDM, orthogonality of the sub-carriers prevents the data streams from interfering with each other. Orthogonality is guaranteed by choosing the frequency spacing of the subcarriers to be equal to the reciprocal of the symbol duration so that the spectra of the subcarriers can still overlap without causing interference. This yields N subcarrier frequencies

$$f_k = k\Delta f,\ k = 0,..,N-1, \tag{3.1}$$

where $\Delta f = f_s/N = 1/NT$ is the frequency spacing and $f_s = 1/T_s$ is the data symbol rate. Based on these definitions, any two distinct subcarriers are orthogonal in the sense that [24]

$$\frac{1}{T_s}\int_{t_0}^{t_0+T_s} e^{j2\pi f_k t} e^{-j2\pi f_\ell t} dt = \frac{1}{T_s}\int_{t_0}^{t_0+T_s} e^{j2\pi(k-\ell)\Delta f t} dt = \begin{cases} 1 & \text{if } k = \ell \\ 0 & \text{if } k \neq \ell \end{cases}. \tag{3.2}$$

Typical subcarrier waveforms in the time and frequency domains are depicted in Figure 9. Note that the subcarriers present in an OFDM system are harmonically related in the time domain. In addition, orthogonality can also be observed in the frequency domain, where the peak of one subcarrier is located at the sidelobe nulls of all other subcarriers and the sidelobes are caused by the Fourier transform (FT) of the rectangular data window.

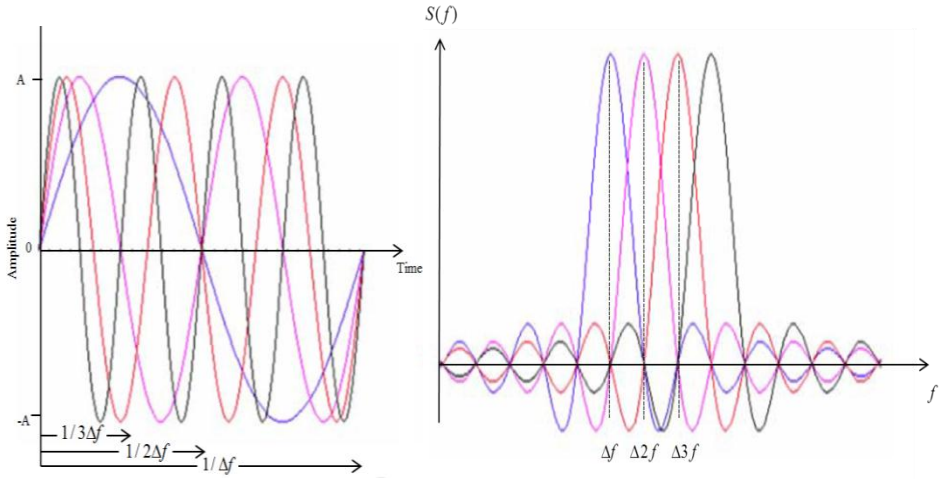

Figure 9. Time-domain and frequency-domain waveform of OFDM (from [25]).

The general idea behind OFDM is to split the total available bandwidth B into N narrowband subcarriers with the same frequency spacing $\Delta f = B/N$ so that the single high-rate data stream is then divided into many lower-rate data streams in the sub-channels. Each subcarrier is modulated individually at different subcarrier frequency $f_k = k\Delta f$ and transmitted simultaneously in a superimposed and parallel form.

This process is illustrated in Figure 10 where R_s is the symbol rate of the input data stream, R_{sb} represents the data rate of each subcarrier, N is the number of subcarriers, and f_k is the k^{th} subcarrier frequency with k in the range $0,...,N-1$. The serial-to-parallel (S/P) block takes a serial stream of data symbols at rate R_s symbols/sec

and rearranges it into N parallel sub-streams of data, each one at a rate equal to R_s/N symbols per second. The implementation of S/P is illustrated in Figure 11.

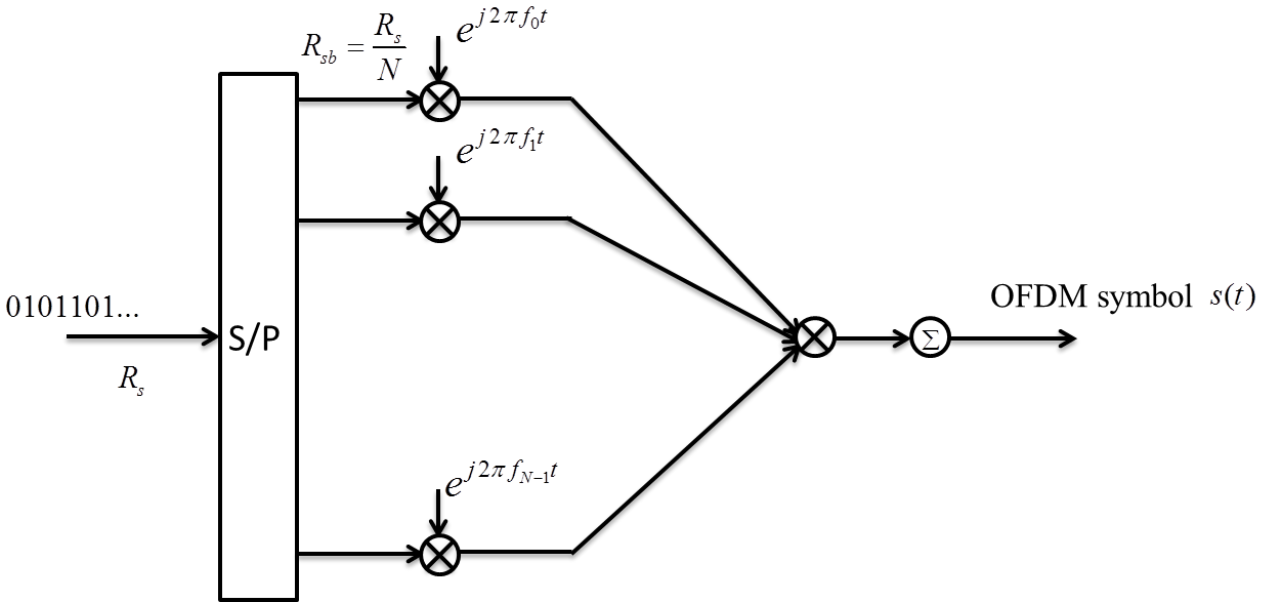

Figure 10. OFDM modulation block diagram (after [26]).

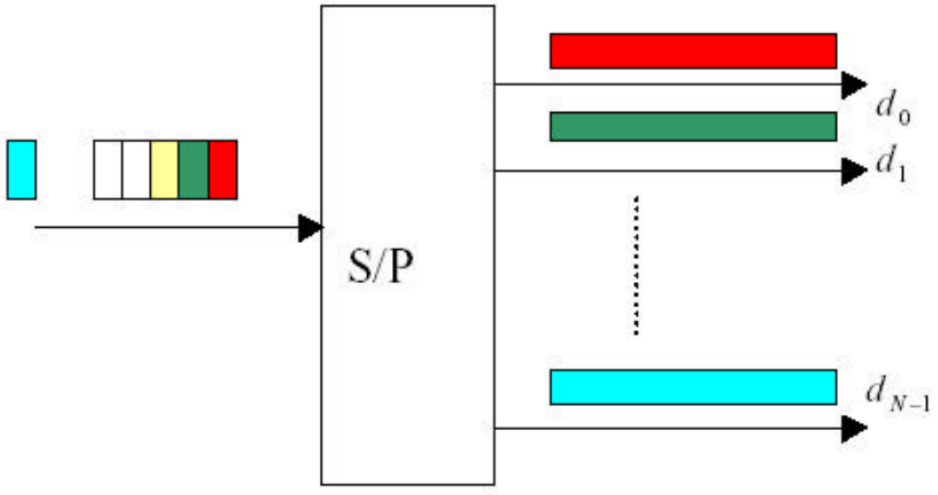

Figure 11. Serial-to-parallel implementation block diagram (from [26]).

With the given choice of subcarrier frequencies discussed previously, it can easily be shown that the OFDM modulation diagram in Figure 10 can be efficiently implemented blockwise using an inverse FFT (IFFT) operation. In fact, referring to Figure 12, let $x[n]$ be the transmitted symbol sequence, and let $X_k[m]$ be defined as the data in the m^{th} data block as $X_k[m] = x[mN+k]$ with $k = 0,\ldots,N-1$; then, the OFDM modulated sequence is given by

$$s[mN+n] = \sum_{k=0}^{N-1} X_k[m] e^{j\frac{2\pi}{N}nk} = IFFT\{X_k[m]\}, \text{ for } k = 0,1,\ldots,N-1. \qquad (3.3)$$

A guard interval is inserted between two successive OFDM symbols to prevent interference due to potential channel-time spreading effects. Further details regarding the concept of the guard interval are provided in the following subsection. Next, the resulting time-domain data that includes the GI are converted back to serial form before transmission. At the receiver, the inverse operation is applied to recover the data.

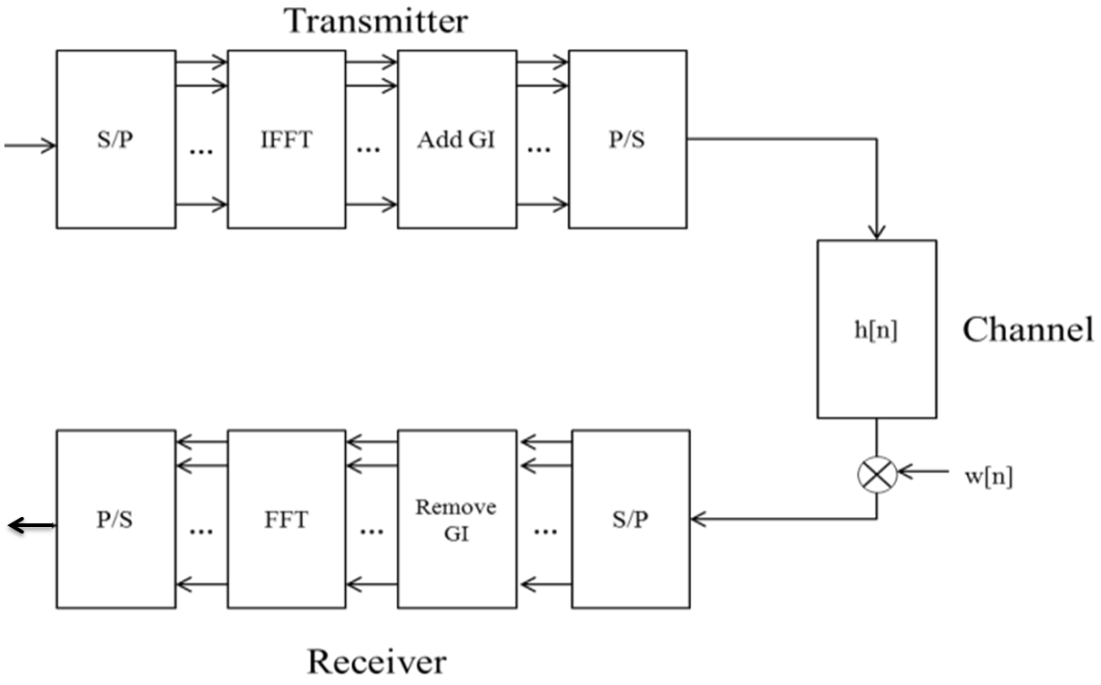

Figure 12. General structure of an OFDM system.

1. Guard Interval (GI)

As discussed in the previous chapter, multipath in wireless communication causes the channel response to spread in time, thus creating ISI. The concept of the guard interval was initially introduced to mitigate ISI. At the receiver, different reflections of the transmitted signal arrive with different time delays due to various obstacles between the propagation paths, and delayed symbol copies may interfere with the next symbol, causing ISI. By properly selecting the duration of the guard interval (T_{GI}) longer than the maximum channel time spread ($\tau_{\max}$), ISI can be eliminated when a GI is inserted between two adjacent data blocks. The concept of the GI is shown in Figure 13(a), while the influences of channel delay spread due to multipath propagation are illustrated in Figure 13(b) and Figure 13(c). As can be seen, ISI only happens when the maximum channel time spread is larger than the guard interval.

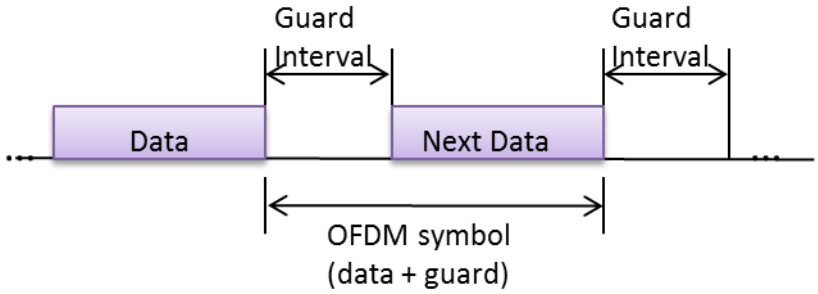

(a) General OFDM symbol structure.

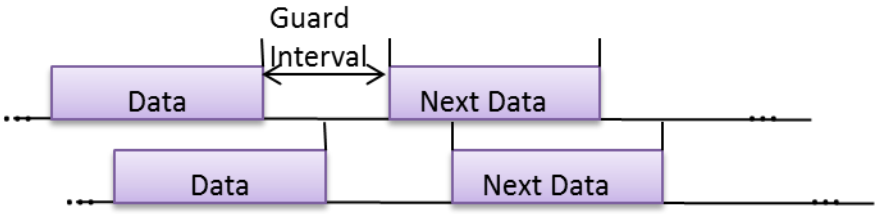

(b) No ISI ($T_{GI} > \tau$).

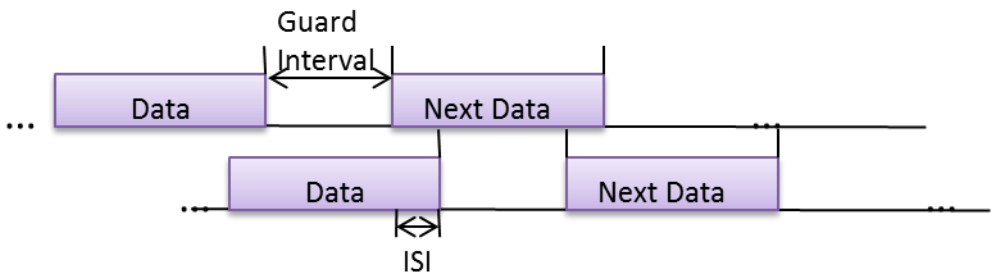

(c) ISI ($T_{GI} < \tau$)

Figure 13. Guard interval elimination of ISI.

2. Types of OFDM

Based on the information transmitted in the GI, several kinds of OFDM systems can be defined. In most OFDM implementations there are three main choices: CP-OFDM with cyclic prefix (CP), TDS-OFDM (time domain synchronous) with pseudorandom noise (PN) prefix and ZP-OFDM with zero prefix (ZP). Most wireless communications and wireless broadcasting implementations use CP-OFDM, which can be considered as the "classic" version of OFDM with the lowest complexity. In recent years TDS-OFDM has been introduced, especially for TV broadcasting in the P.R.C. [27].

a. CP-OFDM

In traditional OFDM, a cyclic prefix (CP) is inserted as the guard interval between nearby OFDM symbols. To cope with time dispersion due to the multipath, the length of the CP must be longer than the time spread of the channel. Since the CP constitutes overhead, its length L, in number of samples, must be much smaller than the length N of the data block. This OFDM technique is referred to as CP-OFDM and has been adopted in most OFDM applications, including the various standards IEEE802.11, 802.16 and also in the European terrestrial television broadcasting standard, DVB-T. An example of CP in OFDM modulation is shown in Figure 14.

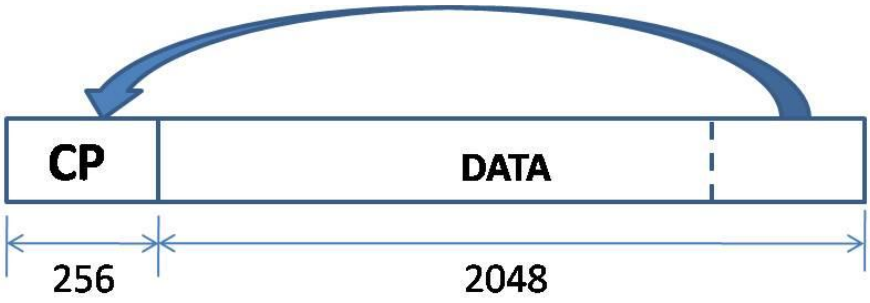

Figure 14. Example of cyclic prefix (CP) in OFDM modulation (from [28]).

The example in Figure 14 shows an application in the European digital broadcasting standard, where the CP-OFDM frame has 2,048 data symbols, and the GI has 256 symbols, as illustrated in Figure 14. As can be seen, 1/8 of the OFDM frame is repeated at the beginning of each frame as a guard interval to avoid interference between frames due to potential multipath problems in the wireless environment and also to facilitate the FFT operation in the demodulation process [28].

This fractional repetition of the OFDM frame in the GI is called the cyclic prefix, which is the most common "classic" OFDM implementation feature in wireless communication standards, such as WiFi, WiMax, or LTE.

The main advantage of the CP-OFDM scheme is a simple demodulation process implemented using a one-tap frequency domain equalizer at the receiver. The use of longer CP sequences to combat the multipath delay, however, causes a loss of channel utilization. Moreover, if there is a need to provide continuous synchronization and channel estimation, as in the case of digital broadcasting DVB-T, some of the subcarriers have to be reserved as pilots inserted as training symbols for synchronization and channel estimation, which leads to significant reductions in the channel throughput.

b. TDS-OFDM

In time-division synchronization OFDM (TDS-OFDM), the transmitted symbols are still processed blockwise by the IFFT in the same way as that used in the conventional CP-OFDM scheme. In the guard interval section, however, a PN sequence is transmitted, which serves as training symbols for channel estimation. Since this PN

sequence is known at the receiver and transmitted periodically, it provides very fast channel estimation and tracking, thus making it attractive in mobile applications. Consequently, in TDS-OFDM there is no need to insert additional training symbols for synchronization and channel estimation, which leads to higher spectral efficiency and system throughput than what may be observed with CP-OFDM. As mentioned before, the main application of this technique is in digital broadcasting for the recently proposed DTTB standard for the People's Republic of China, developed by Tsinghua University [29].

The TDS-OFDM scheme replaces the CP with a PN sequence as guard interval so that the circularity property of the whole CP-OFDM signal frame no longer holds, making the demodulation process in TDS-OFDM systems more complex than in CP-OFDM based systems. Instead, other operations must be employed to preserve the periodic property in order to have simple implementation of demodulation and equalization at the receiver as the CP-OFDM does. The detailed structure and implementation of the TDS-OFDM is provided in Chapter IV.

B. OFDM-BASED DIGITAL TV TERRESTRIAL BROADCASTING TRANSMISSION STANDARDS

Among the four existing DTTB standards, only ATSC adopted in North America is not an OFDM-based technique. The European standard, DVB-T, and ISDB-T employ CP-OFDM, while the P.R.C.'s DTMB utilizes TDS-OFDM. Only the two OFDM-based television standards, DVB-T and DTMB, are discussed in this work, as the goal is to evaluate and compare OFDM-based performance.

1. DVB-T

Digital video broadcasting-terrestrial (DVB-T) is the most widely used European-based standard for DTV transmission; it was first introduced in 1997 [30]. This OFDM-based modulation scheme enables a more efficient use of the available radio frequency spectrum than previous analog transmission schemes. It uses an 8 MHz channel with a choice of coding and modulation parameters set to adapt to various multipath and SNR conditions. General DVB-T structure and modulation parameters are shown in Figure 15.

This system transmits digitized video, audio signal, and other types of data in a compressed format, typically of type MPEG4, using coded orthogonal frequency division multiplexing (COFDM or OFDM) modulation.

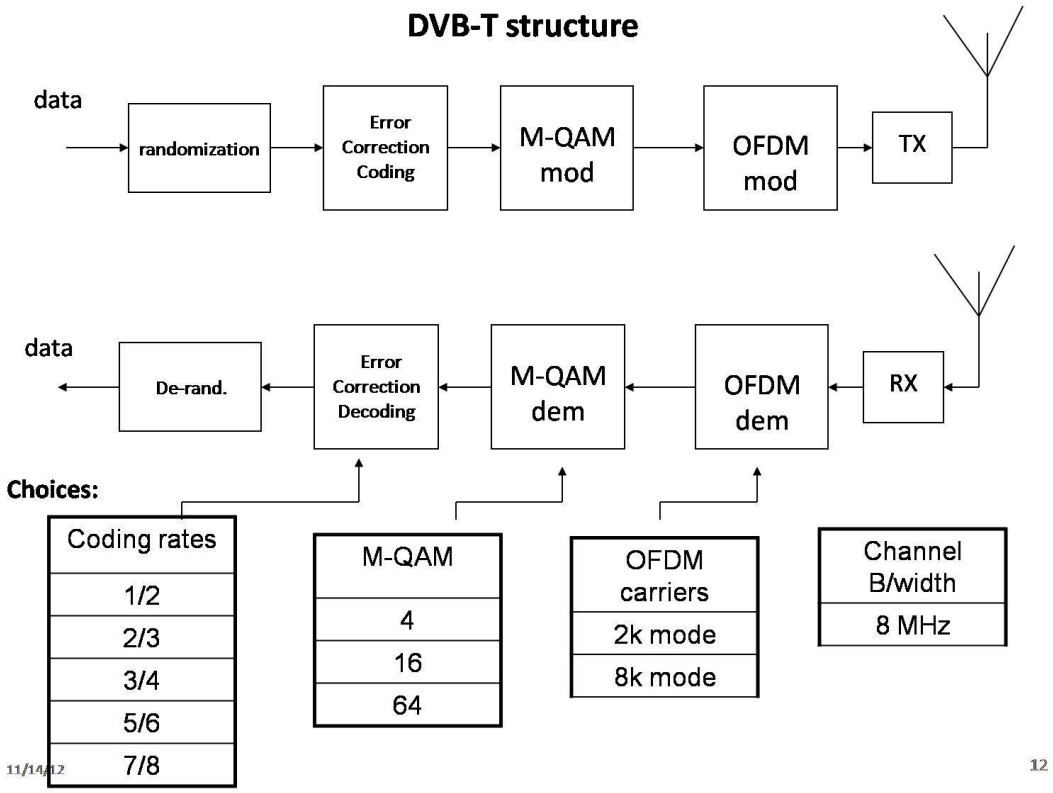

Figure 15. Modulation/demodulation structure of the DVB-T standard and associated modulation parameter choices (from [17]).

a. DVB-T Transmission Parameters

Instead of using a single carrier to carry data streams on one channel, DVB-T utilizes the OFDM multicarrier transmission modulation scheme. Depending on transmission requirements, the number of subcarriers in DTB-T varies between 2,048 (2k mode) and 8,192 (8k mode); these subcarriers are used to carry both data and synchronization symbols. Three different M-QAM modulation options (QPSK, 16-QAM, and 64-QAM) can be selected according to different multipath and SNR conditions. Note that the description shown here represents only a portion of the possible choices, and it is possible to consider other transmission parameters for better transmission performance.

Complete reference information is provided in the ETSI reports [31], [32], and [33]. According to the standard, possible parameter choices of DVB-T are provided in Table 1.

Table 1. Parameters of DVB-T (from [34]).

Nb. of active subcarriers		1705 (2K mode), 6817 (8K mode)
Length of GI (Fraction of useful data length)		1/4, 1/8, 1/16, 1/32
Mapping		QPSK, 16QAM, 64QAM (optionally hierarchical)
Coding	Outer	Reed-Solomon RS(204, 188, t=8)
	Inner	Convolutional code with code rate 1/2, 2/3, 3/4, 5/6, 7/8
Interleaver	Outer	Convolutional interleaving
	Inner	Bitwise + symbol interleaving

b. DVB-T System Description

The data in DVB-T are transmitted as frames. A group of 68 OFDM symbols forms a frame, and the super frame is formed by groups of four frames plus a synchronization signal as shown in Figure 16. Each OFDM symbol carries information associated with the subcarrier frequencies. The information consists of digital audio/video compressed data, pilots, transmission parameters signaling (TPS), and nulls. In addition to the data, each OFDM symbol contains pilots, TPS and nulls for synchronization and channel estimation in order to properly set parameters between transmitter and receiver and to avoid interference with adjacent channels, respectively.

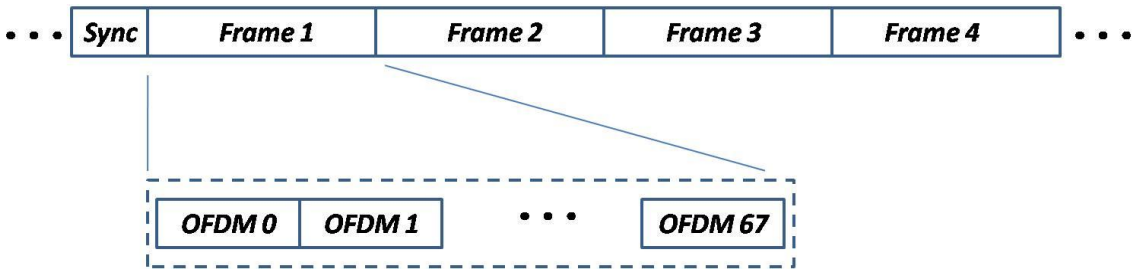

Figure 16. Super frame, frames and OFDM symbols of DVB-T (from [28]).

In the 2k mode OFDM implementation of DVB-T, typically each OFDM symbol has 1,512 data subcarriers, 343 nulls, 176 pilots, and 17 TPS for a total of 2,048 subcarriers. The distribution of pilot subcarriers changes cyclically from OFDM symbol 0 to OFDM symbol 67, as shown in Figure 17 [31], [32], [33]. As a result, the receiver can easily estimate the channel frequency response with minimal loss of data capacity because the pattern of the pilots is known at the receiver.

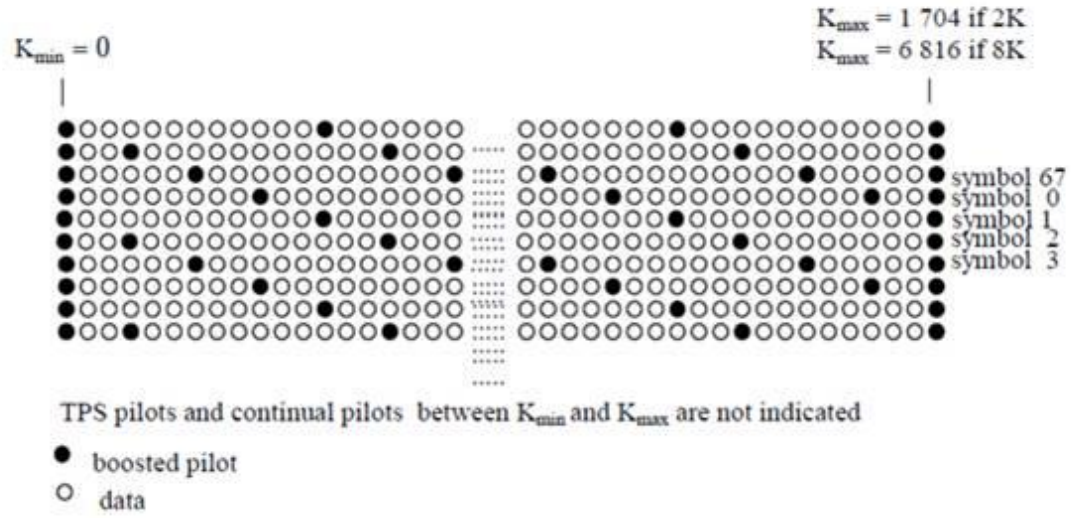

Figure 17. OFDM symbols 0–67 showing pilots and data (from [31]).

2. DTMB

The DTTB standard in the P.R.C., digital terrestrial multimedia broadcasting (DTMB), was ratified in 2006 and became a national standard in 2007 [29]. Instead of the classic CP-OFDM approach used in DVB-T, DTMB adopts the TDS-OFDM modulation scheme that offers the advantage of spectral efficiency and higher system throughput than

those obtained with CP-OFDM. The DTMB transmission parameters are provided in this section, while the details of the system description and prefix structure are explained further in the next chapter.

DTMB consists of single-carrier modulation mode ($C = 1$) and multicarrier modulation mode ($C = 3780$). To evaluate the performance of DVB-T and DTMB schemes, DTMB with multicarrier modulation mode is focused on in this thesis. To be well suited in a wide range of environmental conditions, DTMB has a flexible choice of parameters for modulation types, coding rate, and guard interval ratio to adapt to various situations. DTMB parameters used for the two modulation modes, as well as the parameter comparison between DVB-T and DTMB, are listed in Table 2 and Table 3, respectively.

Table 2. Parameters of DTMB for single-carrier mode and multicarrier mode (from [34]).

		Single-carrier mode	**Multicarrier mode**
Origin		Former ADTB-T	Former DMB-T
Number of subcarriers		C = 1	C = 3780
PN sequence Frame Header	Length	595 (1/6)	420 (1/4), 945 (1/9)
	Power	Non boost	Boosted by 2
	Phase	Same in a superframe	Different or same
Mapping		4QAM-NR, 4QAM, 16QAM, 32QAM	4QAM, 16QAM, 64QAM
Interleaver		Time domain	Time & Frequency domain
Coding	Outer	BCH(762, 752)	
	Inner	LDPC(7493, 3048), (7493, 4572), (7493, 6096)	
	Code rate	0.4(7488, 3008), 0.6(7488, 4512), 0.8(7488, 6016)	

Table 3. Parameter comparison between DVB-T and DTMB (from [34]).

	DVB-T		**DTMB**
	2K mode	***8K mode***	***C = 3780***
FFT size	2 048	8 192	3 780
Nb. of subcarriers	1 705	6 817	3 780
Nb. of data subcarriers	1 512	6 048	3 744
Subcarrier spacing	4 464 Hz	1 116 Hz	2 000 Hz
Signal bandwith	7.61 MHz	7.61 MHz	7.56 MHz
OFDM symbol duration	224 µs	896 µs	500 µs
Power efficiency factor	0.66 (GI=1/4), 0.73 (GI=1/8), 0.77 (GI=1/16), 0.79 (GI=1/32)		0.66 (GI=1/4), 0.81 (GI=1/9)

The details of modulation and demodulation of TDS-OFDM systems are introduced in the next chapter. The key point is that the synchronization signal inserted between OFDM frames can be very effective for rapid synchronization and channel tracking of highly mobile systems.

THIS PAGE INTENTIONALLY LEFT BLANK

IV. TIME-DIVISION SYNCHRONIZATION (TDS) OFDM

One purpose of this thesis is to study the performance of a particular class of OFDM, called TDS-OFDM, currently implemented for digital TV broadcasting in the P.R.C. In our research we have developed generic Simulink-based transmitter and receiver models used in TDS-OFDM to evaluate and compare its performance against that obtained with DVB-T schemes. The TDS-OFDM parameters specifically selected in this work for the evaluation process were those commonly used in DTMB digital broadcasting; the models developed, however, can be used to evaluate any general mobile wireless communication TDS-OFDM-based systems.

First, the structure of the signal frame generated in TDS-OFDM schemes is described. Next, descriptions of the receiver and the transmitter as implemented in Simulink are provided. Two channel models selected for modeling the multipath time-varying channel are introduced and associated parameters provided.

A. TDS-OFDM SIGNAL STRUCTURE DESCRIPTION

In TDS-OFDM-based communication systems, symbols are transmitted in frames, as in the standard OFDM. Each signal frame consists of two parts, the frame head (referred to as frame synchronization) and the frame body, as illustrated in Figure 18.

The frame synchronization provides the information needed for synchronization as well as channel estimation and tracking. Each frame synchronization is generated by PN sequences, which also usually change from frame to frame. Apart from enabling tracking of fast varying channels, the frame synchronization also carries information such as the frame number and possibly timing.

As discussed in the previous chapter, the frame synchronization can be viewed as a GI designed to prevent inter-block interference; its structure is illustrated in Figure 18. It consists of three parts: a preamble, a PN sequence, and a post-amble. The lengths shown in the figure are indicative of a certain specific implementation and can change with different implementations. In the particular DTMB configuration investigated, the PN sequence has a length equal to 255 quadrature phase-shift keying (QPSK) symbols.

The preamble and post-amble sections are the cyclical extensions of the last 83 (preamble) and the first 82 (post-amble) symbols of the PN sequence, as shown in Figure 19. In total, the frame synchronization has a length of 420 symbols. Other values for the preamble L_{pre} (such as 24, 25, 50) and post-amble L_{post} (such as 25, 82, 105, 115) can also be selected depending on the channel maximum delay length.

The second part of the signal frame, the data frame body, has a length of N symbols, which in the DTMB configuration considered here is equal to 3,780. The data frame body has the same length as that selected for the IFFT and FFT operations used in the modulator and demodulator, respectively. Of these N symbols, 3,744 symbols carry the data, and 36 symbols carry transmission parameter signaling (TPS) with all demodulation parameters such as forward error correction (FEC) code rate and interleaver length for the demodulator. Note that this frame contains only the data and the necessary information to recover the data and has no pilot subcarriers since the information required for synchronization and channel tracking is contained in the guard interval. The overall signal frame including frame synchronization and frame body is 4,200 symbols long. The symbol rate of the DTMB is 7.56 MHz, which is the same for both the frame synchronization and the frame body.

Finally, the PN GI power is boosted to twice the power of the frame body in the multicarrier mode configuration employed in the DTMB standard.

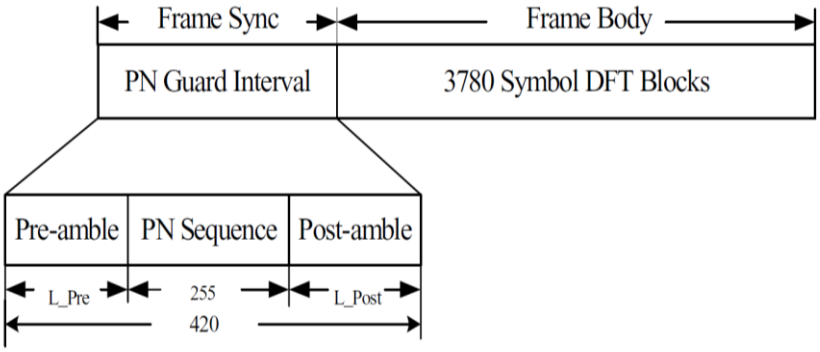

Figure 18. The frame structure of DTMB system (after [35]).

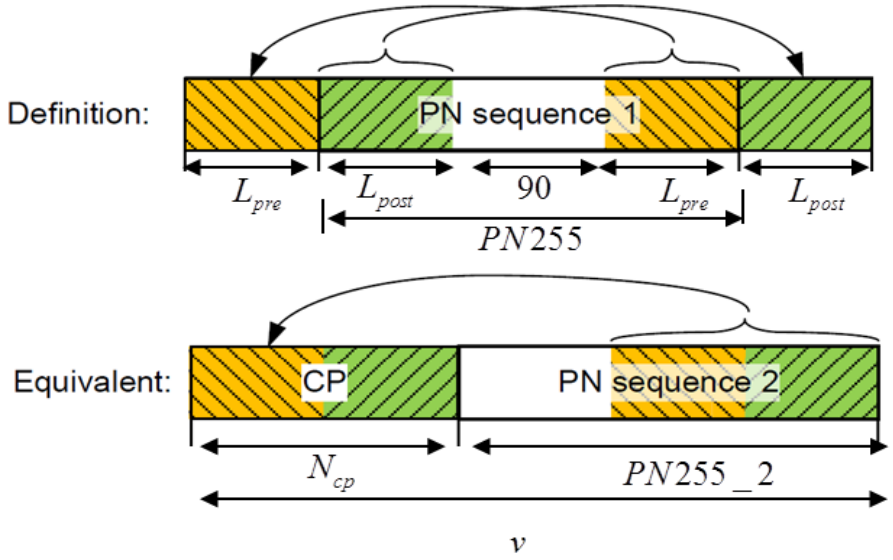

Figure 19. Structure of the GI specified in the DTMB standard (after [36]).

B. TDS-OFDM RECEIVER

At the demodulator, the received signal can be expressed as

$$y(t) = \int_{-\infty}^{t} h(t,\tau)x(\tau)d\tau + w(t), \tag{4.1}$$

where $y(t)$ and $x(t)$ are the time domain received and transmitted signal, respectively; $h(t,\tau)$ is the channel impulse response (CIR) of the frequency-selective time-varying channel, and $w(t)$ represents the AWGN with zero mean and variance equal to 1. Within the i^{th} OFDM frame (GI and data), $x(t,i)$ is defined as the signal transmitted, and the channel is assumed to be time-invariant, with impulse response $h(t,i)$.

At the receiver, time spread in the transmission channel causes ISI between the data frame and the guard interval, as shown in Figure 20. In traditional CP-OFDM, the CP portion of the received signal is discarded, and the rest can be viewed as the circular convolution between the transmitted data and the channel impulse response, as shown in Figure 20(a). Also, the channel is estimated by pilot subcarriers imbedded within the data.

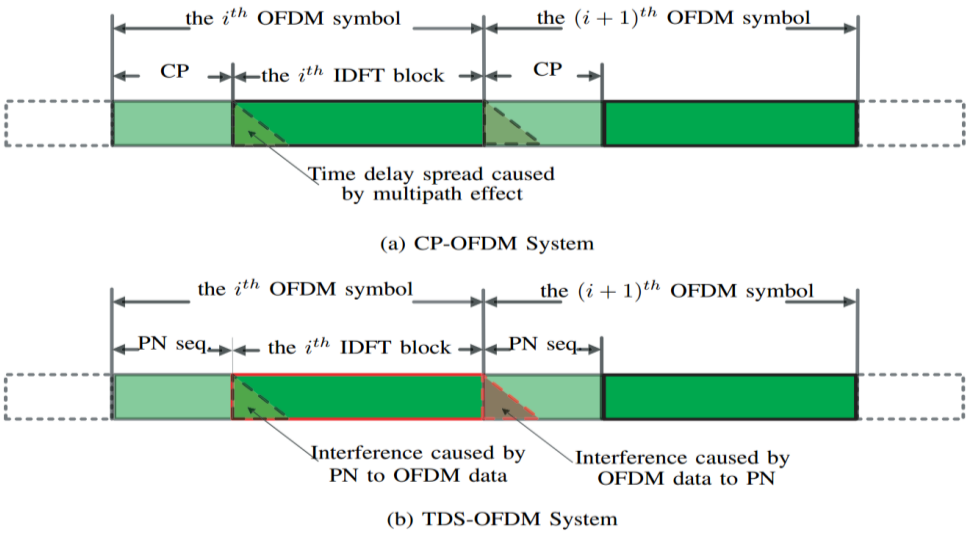

Figure 20. The different impact of ISI in CP-OFDM and TDS-OFDM (from [37]).

For TDS OFDM systems, the structure of the guard interval is shown in Figure 19. The first N_{cp} (83+82) symbols are the repetitions of the last section of the GI. As a consequence, the corresponding received signal can be viewed as the circular convolution between the transmitted PN sequence and the impulse response of the channel as shown in Figure 20(b), and the channel can be estimated by simple FFT operations.

Note that eliminating the first part of the GI guarantees that there is no ISI between successive blocks when the maximum channel delay spread length $\tau_{\max}$ is smaller than the CP length N_{cp}. At that point, the estimated channel frequency response can be computed from the i^{th} OFDM block in the frequency domain as

$$\hat{H}[k,i] = \frac{FFT(y_p[n,i])}{FFT(x_p[n,i])} = \frac{Y_P[k,i]}{X_p[k,i]}, \tag{4.2}$$

where $k = 0,1,...,\mathrm{N}-1$ and $N_{cp} < n < v$, N_{cp} is the length of the CP part of the prefix, v is the length of the PN guard interval, $y_p[n,i]$, $x_p[n,i]$ are the time-domain prefix sequences, respectively, of the received and transmitted signal in the i th block, and $Y_P[k,i]$, $X_P[k,i]$ are the counterparts, respectively, of $y_p[n,i]$, $x_p[n,i]$ in the frequency

domain. The overall Simulink model for the TDS-OFDM receiver is illustrated in Figure 21, while the implementation of the OFDM demodulation and channel estimation is shown in Figure 22. In particular this figure shows the extraction of the GI in the "prefix" block and the channel estimation within the "channel tracking" subsystem. The block called "Pn0inv" carries the vector of terms $1/X_p[k]$ to implement Equation (4.2).

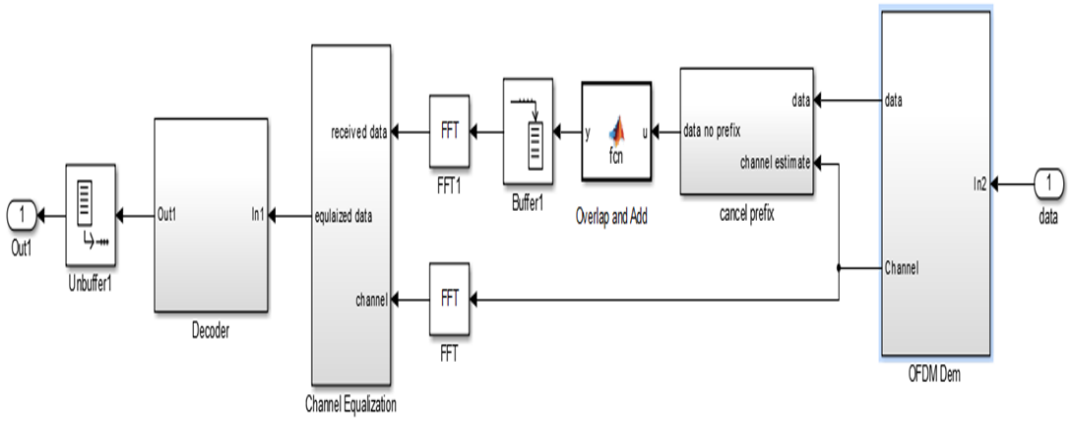

Figure 21. Overall Simulink model of the TDS-OFDM receiver.

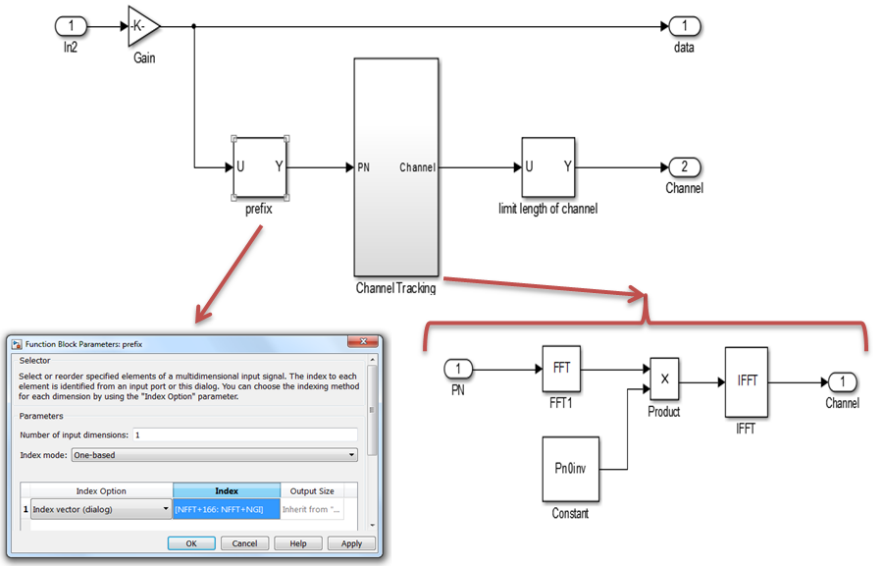

Figure 22. Implementation of the channel tracking in the OFDM demodulation subsystem.

Once the channel impulse response is estimated, the effect of the GI, which is spread in time by the channel, can easily be removed, as shown in Figure 23.

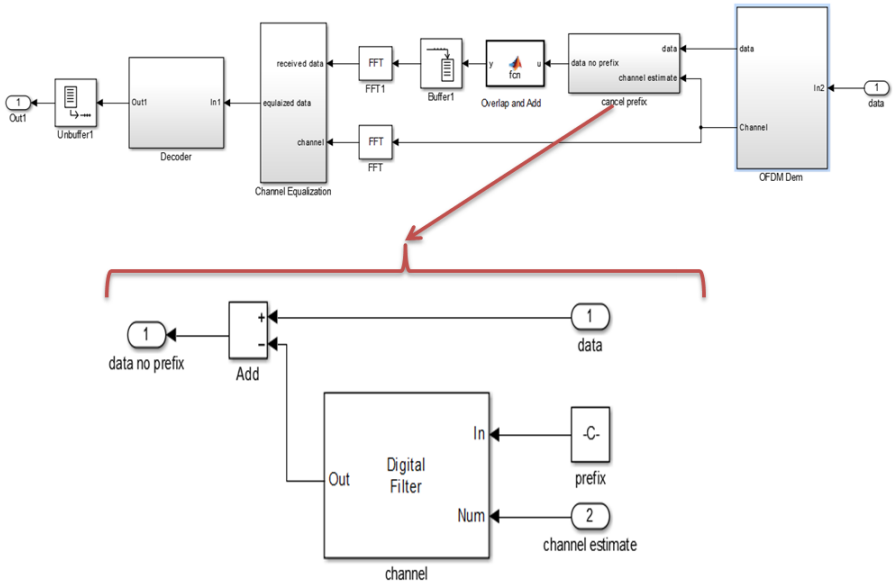

Figure 23. Simulink model of the *cancel prefix* subsystem.

The algorithm is illustrated in Figure 24, where the "shaded triangles" represent the effect of channel spreading at the end of the various blocks. Once the impulse response of the channel is estimated, the effect of the GI can be totally eliminated by convolving the known PN sequence with the channel impulse response. This is subtracted from the received signal so that only the data frame is left, as shown at the end on Figure 24.

As a result, the received data becomes equivalent to that obtained using the zero prefix (ZP) OFDM scheme, where values in the GI are equal to zero, free from interference between data blocks.

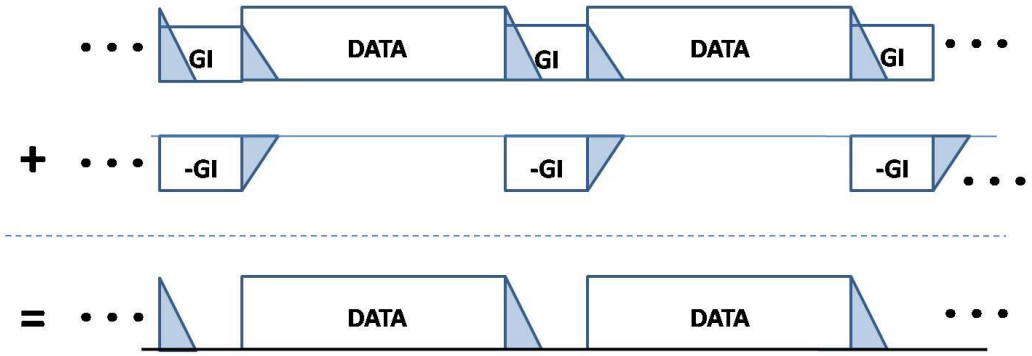

Figure 24. Cancellation of the pseudorandom prefix at the receiver for DTMB standard (from [28]).

Next, an overlap and add (OLA) operation is implemented to discard the guard interval while still preserving the periodic characteristic needed for the FFT operation, as illustrated in Figure 25 [34]. The overall demodulation operation at the receiver consists of the following three steps:

(1) Channel estimation using the received PN sequence.

(2) Cancellation of the pseudorandom prefix: First, convolve the prefix with the estimated channel impulse response, and, next, remove the resultant prefix, as illustrated in Figure 24 where the "shadow" areas represent channel time spreading due to multipath.

(3) "Overlap and Add" operation: as shown in Figure 25, add the tail end of each shadowed data block to the beginning of the same block to preserve the cyclic property that allows for data demodulation using the FFT operation.

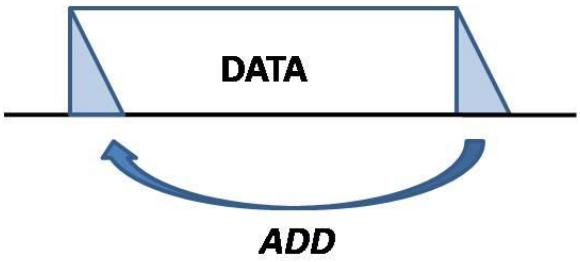

Figure 25. Overlap and add operation at each data block for TDS-OFDM (from [28]).

After the OLA operation is complete, the frequency-domain equalization method used in the CP-OFDM scheme is applied to the resulting TDS-OFDM signal in the channel equalization block. The equalized data can be obtained in the frequency domain by multiplying its Fourier transform with the inverse of the estimated channel frequency response as shown in Figure 26. At that point, the equalized data is demodulated and converted back to binary bits in the decoder Simulink subsystem. Finally, the recovered data are compared to the transmitted data to estimate the BER.

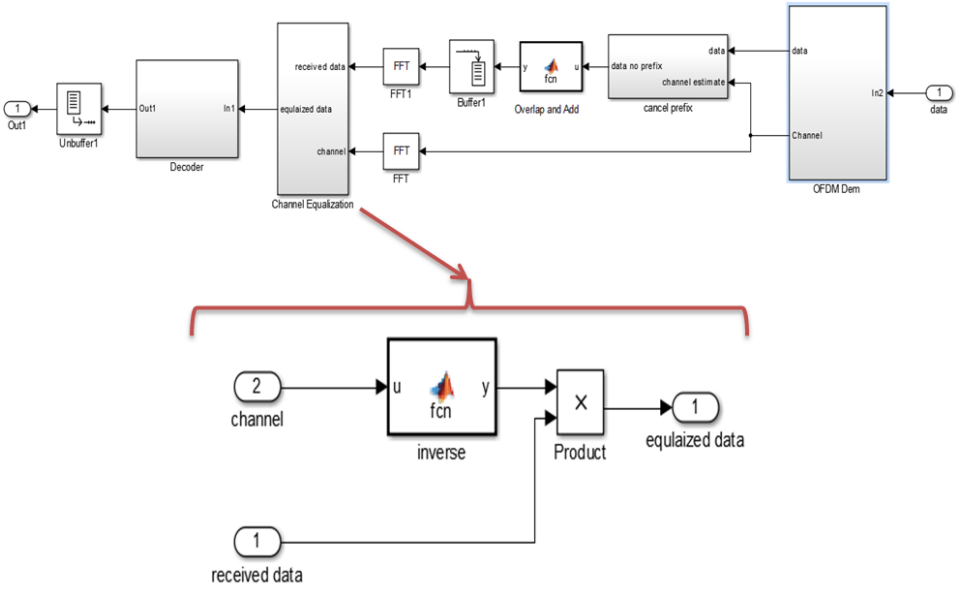

Figure 26. Simulink model for the implementation of the equalization subsystem.

C. TDS-OFDM TRANSMITTER

At the transmitter side, the overall operation implemented in Simulink has three parts: signal generation, M-QAM modulation and OFDM modulation. The binary transmitted signal is first generated using the Bernoulli binary block with equal probability, as shown in Figure 27. Then the modulation technique is applied to the binary transmitted signal by using the rectangular QAM modulator baseband function block. Three modulation schemes, 4-QAM, 16-QAM and 64-QAM, can be selected to

generate the DTMB multicarrier configuration mode. This study selected 16-QAM with a gray code constellation type.

Since data are transmitted in blocks as data frames in OFDM systems, a buffer block must be applied in the Simulink model to enable the N IFFT/FFT operations, as shown in Figure 28. Then, a N point IFFT operation is applied to the modulated data to simulate the serial-to-parallel operation in the OFDM.

The parameters which need to be set for proper operation of the Simulink model are shown in Figure 27 and Figure 28. In particular, the generation of the random data sequence is shown in Figure 27, while the settings for the buffers needed to process the data blocks can be seen in Figure 28.

Finally, the time domain PN guard interval is inserted between two consecutive time domain OFDM data blocks as a guard interval to mitigate the ISI from a previous OFDM block into the next.

The resulting overall transmitted OFDM symbol, also referred to as *superframe*, has a length equal to $P = N + v$, where N and v represent the data length and the guard interval length, respectively. In the DTMB configuration investigated in the study, P is equal to 4,200. The overall simulation model obtained for the TDS-OFDM system is shown in Figure 27, while the overall modulation operation at the transmitter including 16-QAM modulation and OFDM modulation with the PN insertion steps is shown in Figure 28.

The general expression of the transmitted OFDM symbol can be expressed as

$$x[n,i] = \begin{cases} x_p[n,i], & 0 < n < v\text{-}1 \\ x_d[n,i], & v < n < N + v \end{cases}, \tag{4.3}$$

where $x[n,i]$ is the i^{th} time-domain transmitted OFDM symbol with length $P = N + v$, $x_p[n,i]$ is the time-domain PN sequence of length equal to v and $x_d[n,i]$ is the time-domain OFDM data symbol of length equal to N. For simplicity, the parameter n is dropped in the notation for the remainder of this thesis.

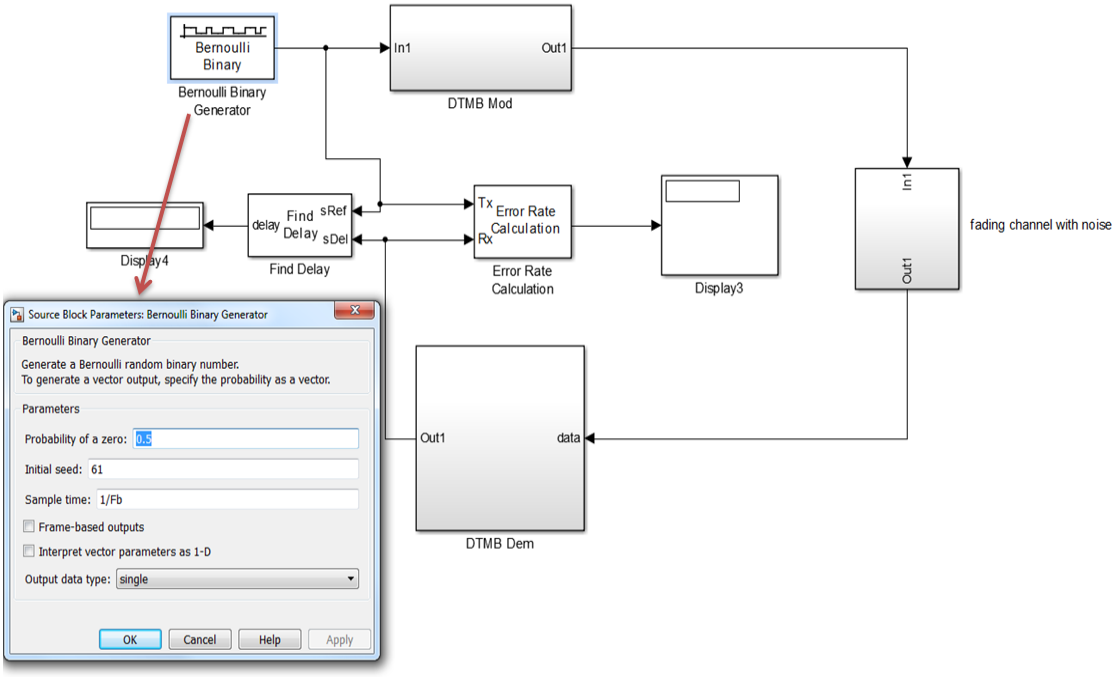

Figure 27. Illustration of the overall communication model and binary transmitted signal generated from the Bernoulli binary function block.

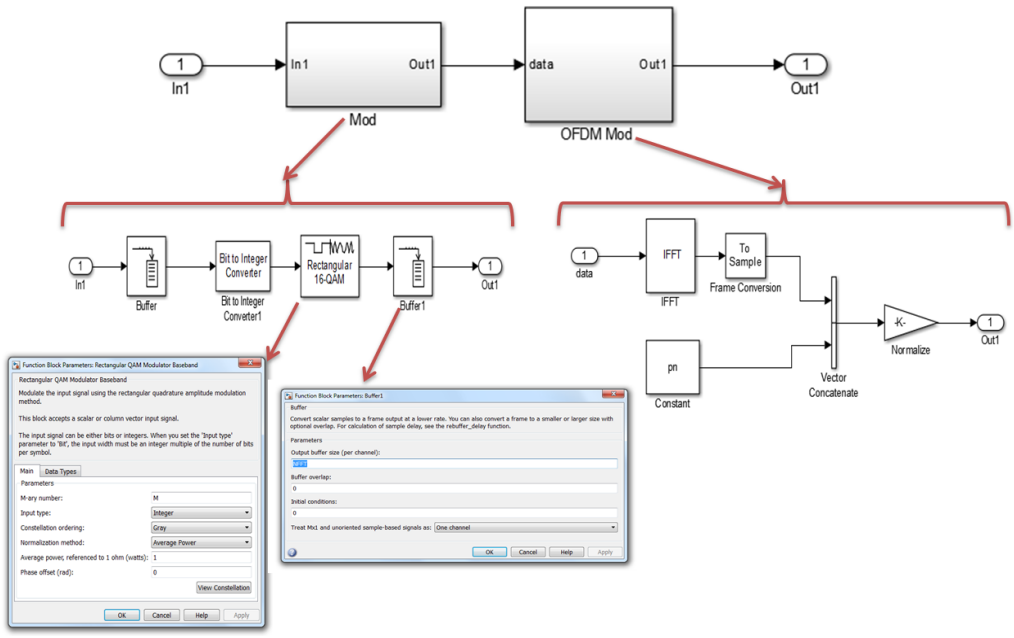

Figure 28. Simulink model of the overall modulation operation at the transmitter with parameters specified in each function block.

D. CHANNEL MODEL FOR SIMULATION

A number of multipath channels with Rayleigh distribution have been chosen to model the multipath propagation in the time-varying scenario for the terrestrial communication channel. In particular two different standard transmission channel models were considered: the COST 207 model with 6-path typical urban (TU6) characteristics and the modified China test8 (CT8) model restricted to the 4-path characteristics only [38], [39]. The power delay profiles of these two channel models are specified in Table 4 and Table 5. Note that care must be taken when selecting channel profiles to ensure complete elimination of ISI, which occurs only when the maximum channel length does not exceed the prefix length.

Table 4. The profile of 6-path typical urban (TU6) channel.

	Tap1	Tap2	Tap3	Tap4	Tap5	Tap6	unit
Delay	0	0.2	0.5	1.6	2.3	5	μs
Power	-3	0	-2	-6	-8	-10	dB

Table 5. The profile of modified China Test 8 (CT8) channel.

	Tap1	Tap2	Tap3	Tap4	unit
Delay	0	0.15	1.8	5.7	μs
Power	0	-20	-20	-10	dB

The multipath Rayleigh fading channel function block was chosen to simulate the channel with multipath characteristics, as copies of the delayed transmitted signal arrive at the receiver with different delays and magnitude attenuation. The number of delay paths and the average path gain were specified in this function block according to the channel model considered.

In addition, three values of maximum Doppler frequency shift $f_{D\max}$ were selected as 2, 40, and 80 Hz to simulate the relative movement between the transmitter and the receiver. These Doppler shift values correspond to a relative velocity of 2.5, 50, and 100 km/h, respectively, assuming the carrier frequency is equal to 860 MHz in the

UHF band. These $f_{D\max}$ values were entered as input parameters in the multipath channel function block. Next, AWGN was added to the multipath Rayleigh channel to account for the noise inherent in a communication channel. The simulation of AWGN was implemented via different values of signal-to-noise ratio per bit (E_b/N_0) to simulate the various channel environment situations from 0 to 50 dB.

Throughout the simulations, the channel was assumed to be time-varying but slow fading, which means the channel response remains nearly constant within one OFDM symbol duration. The multipath time varying channel can be specified as

$$h(t,\tau)=\sum_{i=0}^{L-1}A_i(t)\delta(\tau-\tau_i)\,, \tag{4.4}$$

where L is the numbers of delay paths, τ_i is the delay in time and $A_i(t)$ is the time varying complex gain of i^{th} delay path. The overall Simulink-based channel model including AWGN distortion is shown in Figure 29. In particular the parameters for the simulation are shown in Figure 29.

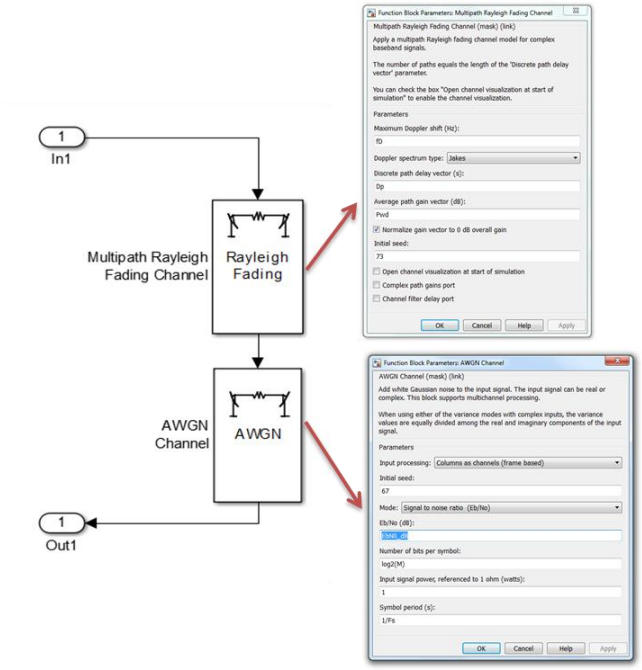

Figure 29. Simulink model of the multipath Rayleigh fading channel and AWGN with parameters specified in each function block.

Simulation results are presented in the next chapter, where comparisons with classic CP-OFDM are made on the basis of BER for different SNR levels and Doppler frequency values.

THIS PAGE INTENTIONALLY LEFT BLANK

V. SIMULATION RESULTS

The fundamental description and implementation of TDS-OFDM was provided in the previous chapter. The simulation results of the TDS-OFDM-based DTTB system, currently applied in DTMB in the P.R.C., with particular attention to its behavior in the presence of a time-varying multipath channel, are presented in this chapter. The system performance is evaluated on the basis of the BER for different SNR levels.

First, the simulation model parameters are introduced, and following that, simulation results are analyzed. Finally, DTMB-based results are compared to those obtained using the counterpart CP-OFDM scheme employed in the European DVB-T.

A. SIMULATION PARAMETERS OF THE TDS-OFDM-BASED DTTB SYSTEM

The DTMB-based simulation parameters are listed in Table 6. As discussed earlier, OFDM is a special case of the MCM scheme that splits the total bandwidth B into N orthogonal subcarriers with the same frequency spacing ($\Delta f = B/N$). Assuming an 8.0 MHz channel bandwidth, a sampling rate of 7.56 MHz and 3,780 subcarriers were chosen for the simulation, in line with standard broadcasting applications. Using these parameters, we set the data frame body to 500 μs, while the PN prefix was selected as 1/9 of the OFDM data portion that provides the guard time equal to 55.6 μs. Therefore, the duration of the total OFDM symbol was set to 555.6 μs.

Table 6. Simulation parameters of the TDS-OFDM based DTTB system.

Channel bandwidth	8 MHz
Signal bandwidth	7.56 MHz
Frame body length(FFT size)	3,780 (3,744 data+36 TPS)
Frame body period	500 μs
Subcarrier frequency spacing	2k
Frame heather length	420 (1/9 of 3780)
PN sequence length	255
Pre-amble length	83
Post-amble length	82

B. PERFORMANCE EVALUATION OF TDS-OFDM IN DTMB

The TDS-OFDM-based DTTB system performance using a 16-QAM modulation scheme was evaluated in terms of BER versus SNR level for SNR values ranging from 0 to 50 dB. For simplicity, all simulations conducted in this thesis assume perfect timing and frequency synchronization. In addition, the channel models are selected with the maximum delay path not exceeding the GI length, and the channel is assumed to be time-invariant within one OFDM symbol duration. The total length of the data in the simulation was set to 5×10^{7} symbols in this research.

As shown in Figure 30 and Figure 31, the BER performance of the TDS-OFDM-based DTTB system, DTMB, in TU6 and modified CT8 channel, respectively, with maximum Doppler frequency shifts f_d of 2 Hz, 40 Hz, and 80 Hz and the BER for an AWGN channel without multipath or Doppler effect is also provided (pink curve) for comparison purposes.

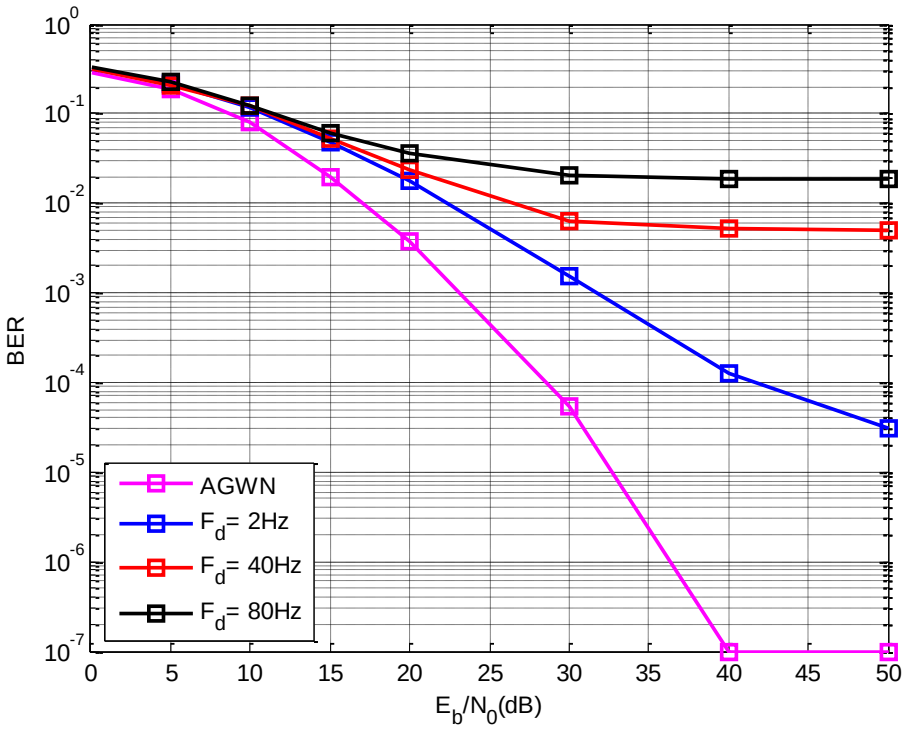

Figure 30. DTMB system BERs over the TU6 channel for various noise and maximum Doppler shift levels.

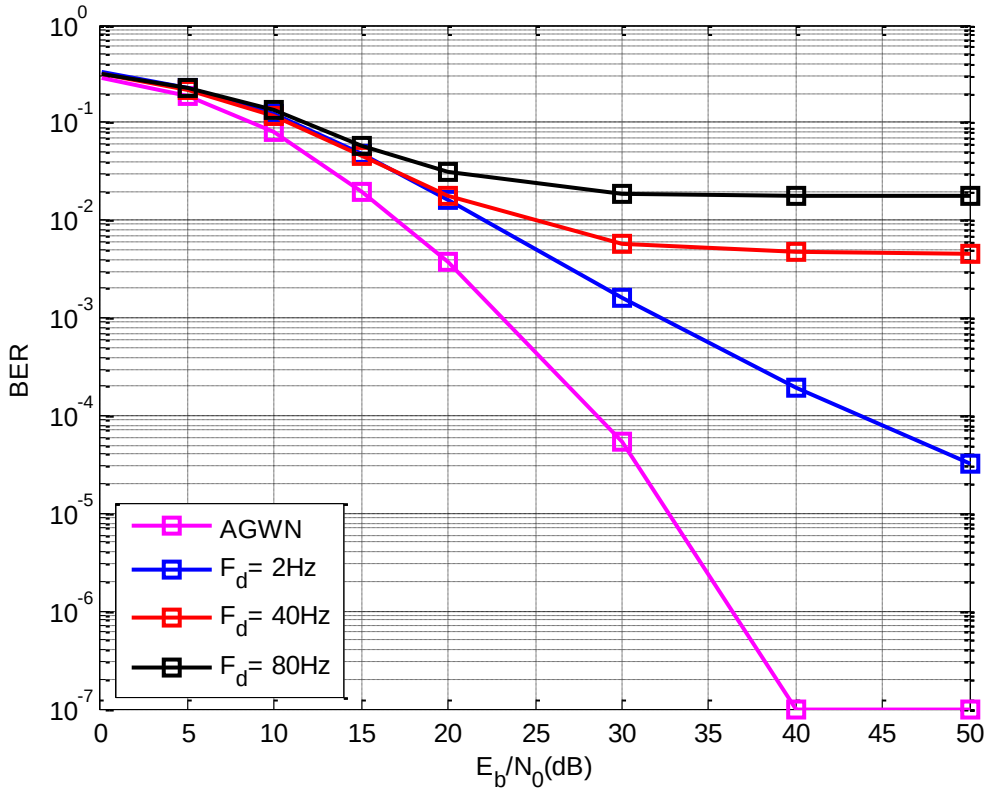

Figure 31. DTMB system BERs over the CT8 channel for various noise and maximum Doppler shift levels.

Results show that the BER values observed in both channel scenarios are almost identical for all SNR levels and Doppler shift values considered. As expected, BER values decrease as the SNR level increases or the maximum Doppler shift value decreases, as illustrated in Figure 30 and Figure 31.

For example, the BER in the TU6 channel configuration with Doppler shift can improve up to around 3×10^{-5} for a smaller Doppler shift of $f_d = 2$ Hz, while for cases with higher Doppler shifts, such as $f_d = 40$ Hz and $f_d = 80$ Hz, the BER increases to 5×10^{-3} and 1.8×10^{-2}, respectively.

Results indicate that the BER plateaus for 30 dB and larger for high levels of Doppler shifts. Results also show that the BER value decreases to almost zero, indicated

as 10^{-7} in the graphs, when there is no multipath or the transmission channel is time-invariant, as shown in both Figure 30 and Figure 31, for SNR levels above 40 dB.

As expected, the BER worsens in the presence of multipath and time-varying channel conditions such as in the chosen TU6 or modified CT8 channel models.

An initial assessment tool of the model implemented was done by plotting the subcarrier constellations obtained at the demodulator stage for different channel conditions with the SNR equal to 50 dB, as shown in Figure 32.

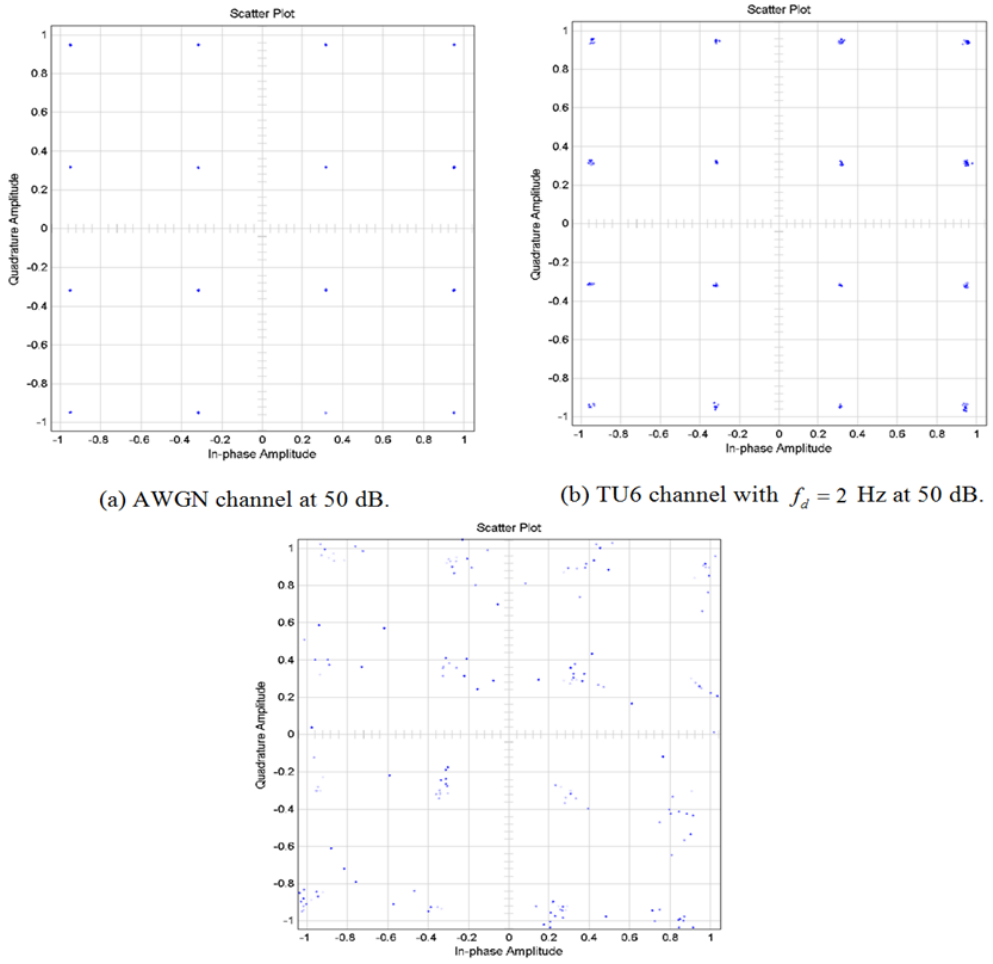

(a) AWGN channel at 50 dB.

(b) TU6 channel with $f_d = 2$ Hz at 50 dB.

(c) TU6 channel with $f_d = 80$ Hz at 50 dB.

Figure 32. DTMB subcarrier constellation at the demodulator in different channel conditions at 50 dB.

From Figure 32(a), it can be seen that in an AWGN-only channel with the SNR equal to 50 dB, the subcarrier constellation obtained at the demodulator with 16-QAM showed perfect 16 fix points with the BER equal to zero. When the channel has multipath, however, and is time-varying, such as the TU6 channel with a maximum Doppler shift equal to 2 Hz, the constellation diagram starts showing perturbations as illustrated in Figure 32(b). Similarly, for the TU6 channel with maximum Doppler shift equal to 80 Hz, the constellation diagram is degraded but still shows the expected 16 clustered data points, as illustrated in Figure 32(c). The data point spreads represent fluctuations in the recovered signal due to the high Doppler shift level. As a result, the BER obtained in this case was much higher and equal to 1.87×10^{-2}. Note that the increase in maximum Doppler shift still results in a high BER even for a large SNR, as expected.

C. PERFORMANCE COMPARISON OF TDS-OFDM VERSUS CP-OFDM IN DTTB

In order to compare the performances of TDS-OFDM-based and conventional CP-OFDM DTTB systems, we simulated both DTMB and DVB-T models in Simulink. Both models were set according to the corresponding standards. We used the CP-OFDM based system implementation in [40]; simulation implementation details for this standard are provided in Appendix B and Appendix C.

Specific implementation parameters selected for the CP-OFDM configuration implemented in the DVB-T standard are as follows. We selected the "2k" mode, which uses 2,048 subcarriers and standard CP-OFDM scheme and boosts the power of the pilot subcarriers by a factor equal to 16/9 as compared to the data subcarriers. The length of the GI was chosen to be 1/32 of the frame body. The sampling rate was selected as 64/7 Hz. To ensure a fair performance comparison, all other parameters were set to be identical to those used in DTMB; the channel bandwidth was selected as 8 MHz, and the frame body modulation scheme was selected as 16-QAM. The resulting DVB-T-based BER performances in TU6 and modified CT8 channel environments with AWGN are included in Appendix D.

The BER comparison between DTMB and DVB-T for both TU6 and modified CT8 channel with different maximum Doppler shifts f_d are shown in Figure 33 and Figure 34, respectively.

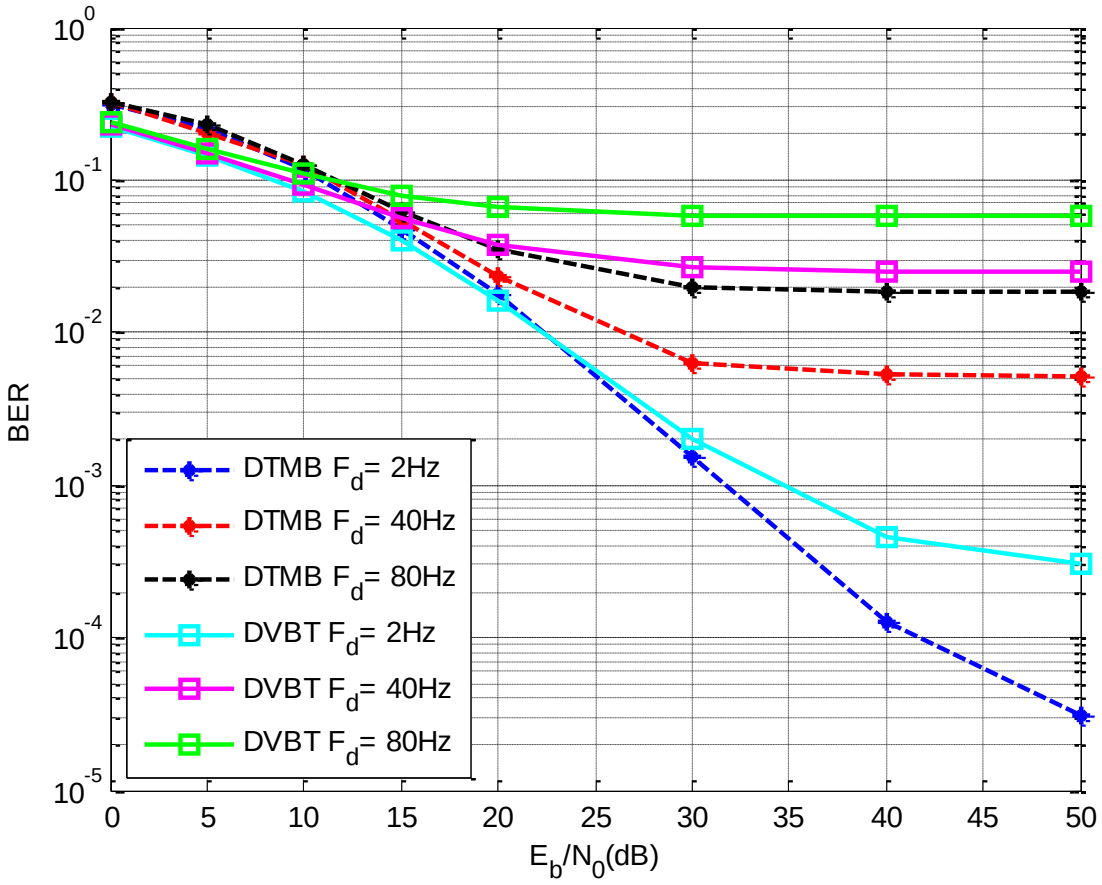

Figure 33. BER comparison between DTMB and DVB-T for TU6 channel with different values of the maximum Doppler shift.

Overall, BER results show similar trends obtained for DTMB and DVB-T in both channel environments considered, as illustrated in Figure 33 and Figure 34.

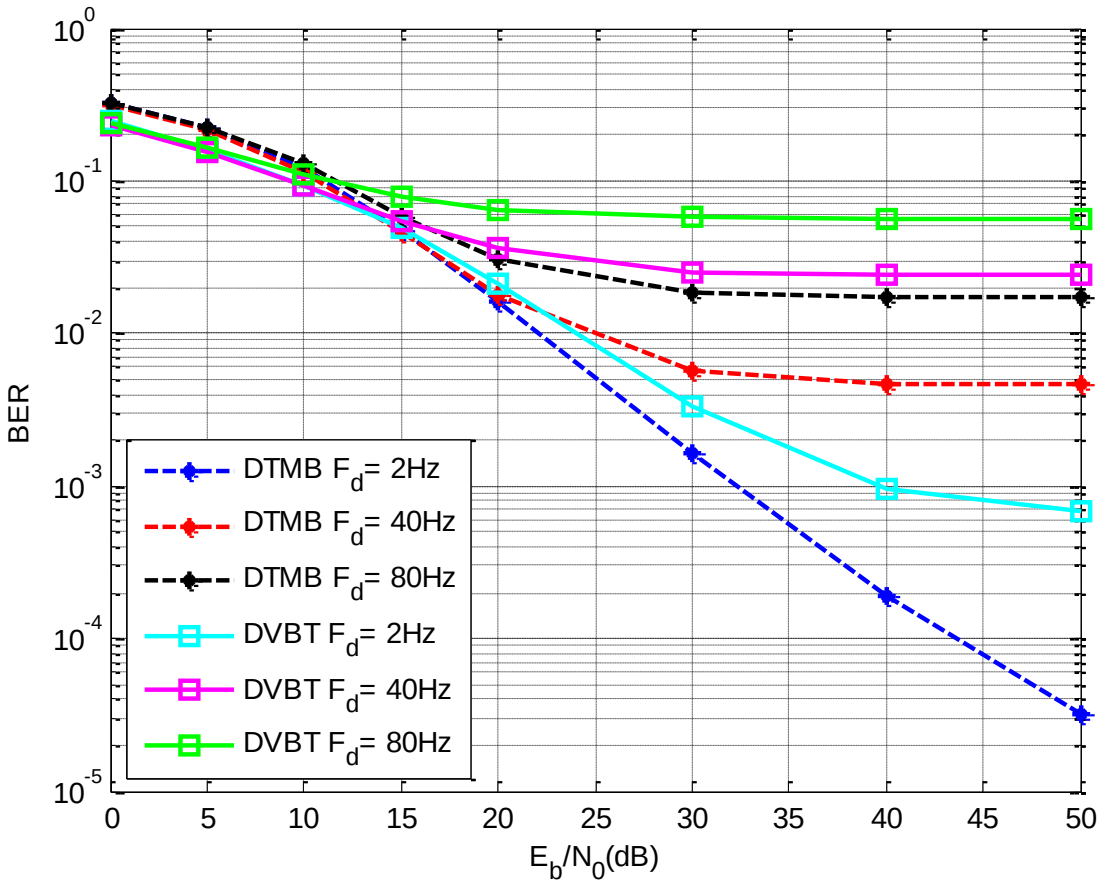

Figure 34. BER comparison between DTMB and DVB-T for modified CT8 channel with different values of the maximum Doppler shift.

Results show significantly lower BERs are obtained with the DTMB standard for SNR levels above around 25 dB for the three considered Doppler shift levels in both transmission channels investigated, as shown in Figure 33 and Figure 34. TDS-OFDM, employed in DTMB, with its boosted PN guard interval and no pilots inserted in the OFDM data portion, is designed to allow for faster channel tracking and better spectral efficiency than the conventional CP-OFDM applied in DVB-T. Results show DTMB is better suited to handle highly mobile environments as BERs obtained for Doppler shifts equal to 80 Hz (100 km/h) are smaller than those obtained for DVB-T at the lower Doppler shift of 40 Hz (50 km/h).

As can be seen from Figure 33, the DTMB system implemented in the TU6 channel environment consistently outperforms DVB-T for SNR levels above 12 dB to 23 dB, where the specific SNR level cross-point depends on the Doppler shift level considered. In addition, we note the BER behavior remains flat for both DTMB and DVB-T implementations for large Doppler level scenarios, while it continues to decrease with increasing SNR levels for low Doppler shift levels. This behavior is expected to improve when FEC coding and interleaver operations are added.

In the CT8 channel case, DTMB outperforms DVB-T for SNR levels above 12 dB to 15 dB, where the specific SNR level cross-point depends on the Doppler shift level considered.

Similar trends for the BER results for both selected channels show the effectiveness of the developed system with the performance of DTMB (TDS-OFDM) better suited for faster time-varying scenarios than DVB-T (CP-OFDM) with the proper SNR level provided.

VI. CONCLUSIONS

A. OVERALL RESULTS

The purpose of this thesis was to model and analyze the performance of the TDS-OFDM system for DTTB for the frequency-selective, slow fading channel scenario. OFDM is known for being effective in frequency-selective fading multipath channels, and the classic CP-OFDM has been applied in many fields of communication such as broadcasting and cell phone application. The newly proposed TDS-OFDM, however, is only adopted in DTMB as the DTV standard of the People's Republic of China and is not yet officially adopted for other communication applications, even though its characteristics make it very well suited to mobile environments. Note that simulation results obtained in this research are not limited to digital broadcasting only but can be extended and applied to any general mobile wireless communication applications.

General characteristics of mobile propagation and types of fading were discussed. Next, the fundamentals of conventional OFDM followed by the newly proposed TDS-OFDM were provided. Finally, the comparison of two OFDM techniques for digital broadcasting was conducted using the proposed Simulink-based models. Two standard channel models, TU6 and modified CT8, were utilized for modeling the multipath Rayleigh fading channel and showing the validity of the proposed model. A physical phenomenon of wireless communication, Doppler shift, was also taken into account for the time-varying scenario. Channel estimation and equalization were implemented at the receiver to recover the transmitted signal. System performance was then evaluated in terms of BER as a function of SNR for different values of maximum Doppler frequency shifts.

In both channel environments, the overall BER results were similar for each maximum Doppler shift case. As expected, the overall BER performance improves with increasing SNR or decreasing Doppler frequency. For lower values of the Doppler frequency such as $f_d = 2$ Hz, the BER is inversely proportional to the SNR. For higher Doppler frequencies such as $f_d = 40$ or 80 Hz, however, the BER improvement is limited

due to the fast variation of the channel as the SNR increases. Results verify that the BER remains larger for poor channel conditions even when the SNR increases. Note that performance improvements can be expected by adding FEC coding and interleaver blocks in the communication system, which are not present in the model derived in the study.

In general, TDS-OFDM outperforms CP-OFDM for a large SNR, i.e., above 20 dB (depending on channel conditions), for both channels and for each corresponding Doppler case. The TDS-OFDM is faster than the CP-OFDM to adapt to changes in the physical time-varying channel, which is reflected in the resulting BER for highly mobile environments.

B. RECOMMENDATIONS FOR FUTURE WORK

There are several areas recommended for follow-on research. All simulations in this thesis were conducted given the assumption of perfect time and frequency synchronization; therefore, errors resulting from phase noise and frequency offset were not taken into consideration, and these may seriously degrade the system performance. It is recommended that timing and frequency offset tracking be implemented to avoid performance degradation due to offset error.

The channel estimation in this research was carried out in the frequency domain using the FFT. Since it is known that accurate channel estimation is crucial in OFDM systems, it would be beneficial to conduct other channel estimation methods that can be found in the research literature, such as time-domain correlation of the PN sequence with the received signal.

Finally, for severe channel conditions such as Rayleigh multipath with large Doppler shift, results showed the system performance cannot be improved with a higher SNR. Therefore, introducing FEC coding with appropriate code rate and interleaver lengths is recommended to improve the overall system performance.

APPENDIX A. MATLAB CODE

The MATLAB code in the callback function of each DTTB model used in Simulink to evaluate the system performance is provided here. The complete Simulink model is available upon request from the author (laihuichen@hotmail.com) or thesis advisor (fargues@nps.edu).

1. Model Initialization Parameters of DTMB in the Callback Function

```
clear all

%parameters needed to reset for different cases:
M=16; % M-QAM
EbN0_dB = 15; %in dB

%Rayleigh Multipath CH with Doppler:
fD = 80; % doppler freq. in (2;40;80)Hz
%for TU6 CH
Dp = [0 0.2e-6 0.5e-6 1.6e-6 2.3e-6 5e-6]; %multipath time delay in (sec)
Pwd = [-3 0 -2 -6 -8 -10 ]; %multipath power in (dB)
%for CT8 CH
%Dp = [0 0.15e-6 1.8e-6 5.7e-6]; %multipath time delay in (sec)
%Pwd = [0 -20 -20 -10 ];
% Frequencies
Fs=(7.56)*1.0e06; % sampling and symbol rate in Hz
NFFT=3780; % FFT length

%compute noise variance according the specified Eb/N0
EbN0 = 10^(EbN0_dB /10); %dimensionless ratio

%Received delay setting in the error rate calculation block
TD=zeros(1,16);
% M=16, 16-QAM
TD(16)=30244;
%M=4, QPSK
TD(4)=15122;
%M=2, BPSK
TD(2)=7560;

%noise variance
Ps = 1; %signal power=unity power=OFDM data power
L = NFFT/9; %prefix length(420)
```

```
N = NFFT; %OFDM data length(3780)
r = 2; %prefix power boost factor
eps = Ps*(1+(L/N)*r)/(log2(M)*EbN0) %noise power (assume zero-mean)

% PN sequence for GI
p0 = sign(randn(1,255)) + 1i*sign(randn(1,255)); %QPSK signal
p0 = p0/(sqrt(NFFT)); %normalized prefix power boosted to twice OFDM data part

pre = p0(255-83+1:255);
post = p0(1:82);
pn=[pre, p0, post];
NGI=255+82+83; % Length Guard Interval
Pn0=fft(pn(166:NGI));
Pn0inv=conj(Pn0)./(abs(Pn0).^2 + eps);
%pn = pn(1:42);
zeropn=[zeros(1,NFFT), pn];

% parameters
Fb=log2(M)*(NFFT/(NFFT+NGI))*Fs; % bit rate
```

2. Model Initialization Parameters of DVB-T in the Callback Function

```
clear all
%parameters need to reset for different cases:
M=16; % M-QAM
EbN0_dB = 10; %in dB

%Rayleigh Multipath CH with Doppler:
fD = 80; % doppler freq. in (2;40;80)Hz
%for TU6 CH
Dp = [0 0.2e-6 0.5e-6 1.6e-6 2.3e-6 5e-6]; %multipath time delay in (sec)
Pwd = [-3 0 -2 -6 -8 -10 ]; %multipath power in (dB)
%for CT8 CH
%Dp = [0 0.15e-6 1.8e-6 5.7e-6]; %multipath time delay in (sec)
%Pwd = [0 -20 -20 -10 ];
%compute noise variance according the specified Eb/N0
%EbN0_dB= 50; %in dB
EbN0 = 10^(EbN0_dB /10); %dimensionless ratio

% Channel Estimation in Freq. Domain
% Frequencies
Fs=(64/7)*1.0e06; % sampling and symbol rate in Hz
Fb=log2(M)*(1512/(2048+64))*Fs; % bit rate

% DVB-T settings:
```

```
% Kdata = data subcarriers (68x1512)
% Kpilots = pilots subcarriers (68x176)
% Ktps = TPS subcarriers (68x17)
% 1512+176+17=1705
% nulls=2048-1705=343

[Kmod, Kdem, Kdata, Xoh, Koh, Nk,NFFT, NCP]=dvbtframe2k;
Kpilots=Koh(:, 1:Nk(2));
Xpilots=Xoh(:, 1:Nk(2));
[KH, XpH, IK, Minv]=channel estimator(Kpilots, Xpilots,NFFT);

%noise variance (account for BOOST pilot)
Ps = 1; %signal power=unity power=OFDM data power
L = NFFT/32; %prefix length
Ndata = 1512;
Ntps = 17;
Npilot = 176;
N = NFFT; %OFDM data length(3780)
r_pilot = 16/9; %pilot power boost factor
r = 1; %prefix power boost factor
G = 1 + (L/(Ndata+Ntps+Npilot*r_pilot));
eps = Ps*G/(log2(M)*EbN0) %noise power (assume zero-mean)

%compute the normalized gain factor K (account for BOOST pilot)
N = NFFT;
Ndata = 1512;
Npilot = 176;
Ntps = 17;
K1 = N/sqrt(Ndata+Npilot*r_pilot+Ntps) %gain factor to normalize total power
```

3. Overlap and Add Operation

```
function y = fcn(u)
%#codegen
 NFFT=3780;
 L=83;
 y=u(1:NFFT);
 y(1:L)=y(1:L)+u(NFFT+1:NFFT+L);  %overlap and add
 % end
```

4. Inverse Operation in the Equalization

```
function y = fcn(u)
%#codegen
y = conj(u)./(npw+abs(u).^2);
%use eps(noise power)in equalization in consistent with CH EST scheme
in simulation
% end
```

APPENDIX B. SIMULATION DIAGRAM OF DVB-T

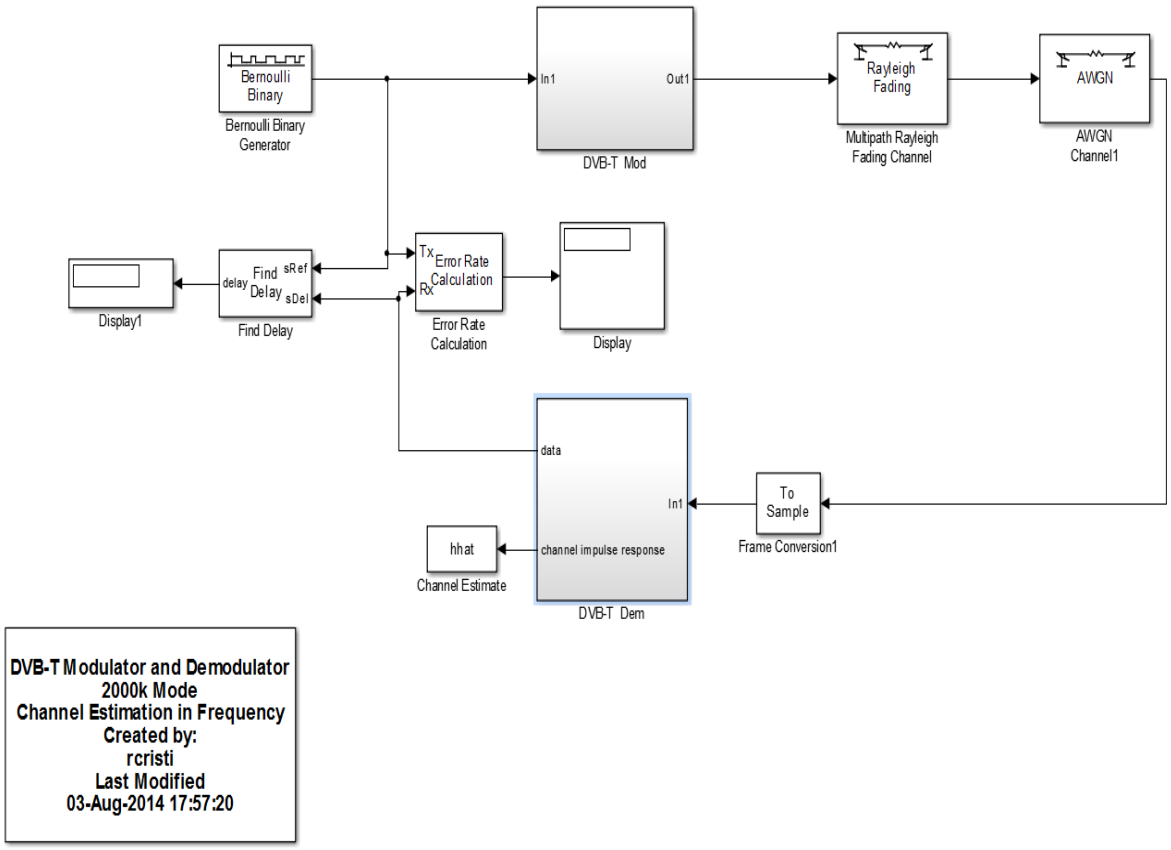

Figure 35. Simulink diagram of the proposed DVB-T (from [40]).

THIS PAGE INTENTIONALLY LEFT BLANK

APPENDIX C. SIMULATION PARAMETERS OF THE DVB-T SYSTEM

Table 7. DVB-T system simulation parameters.

Channel bandwidth	8 MHz
Signal bandwidth	64/7 MHz
Frame body length (FFT size)	2,048 (2k)
Frame heather length	64 (1/32 of 2,048)
Numbers of null subcarriers	343
Numbers of pilot subcarriers	176
Numbers of TPS subcarriers	17

THIS PAGE INTENTIONALLY LEFT BLANK

APPENDIX D. SIMULATION RESULTS OF DVB-T

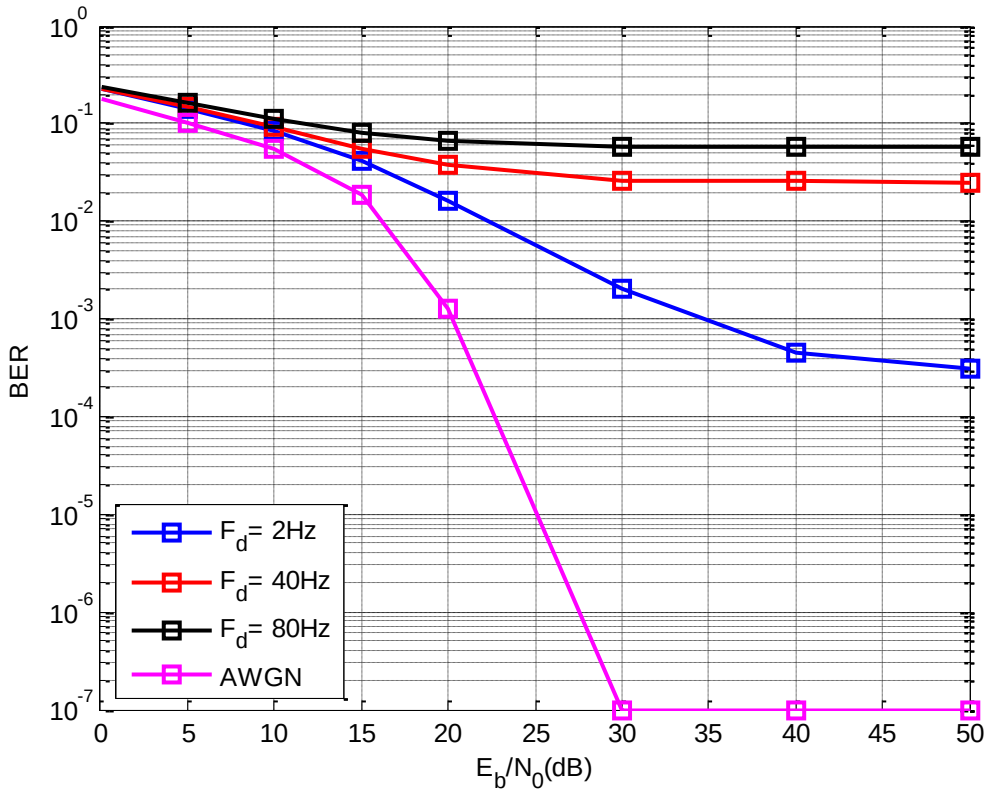

Figure 36. DVB-T system BERs over the TU6 channel for various noise and maximum Doppler shift levels.

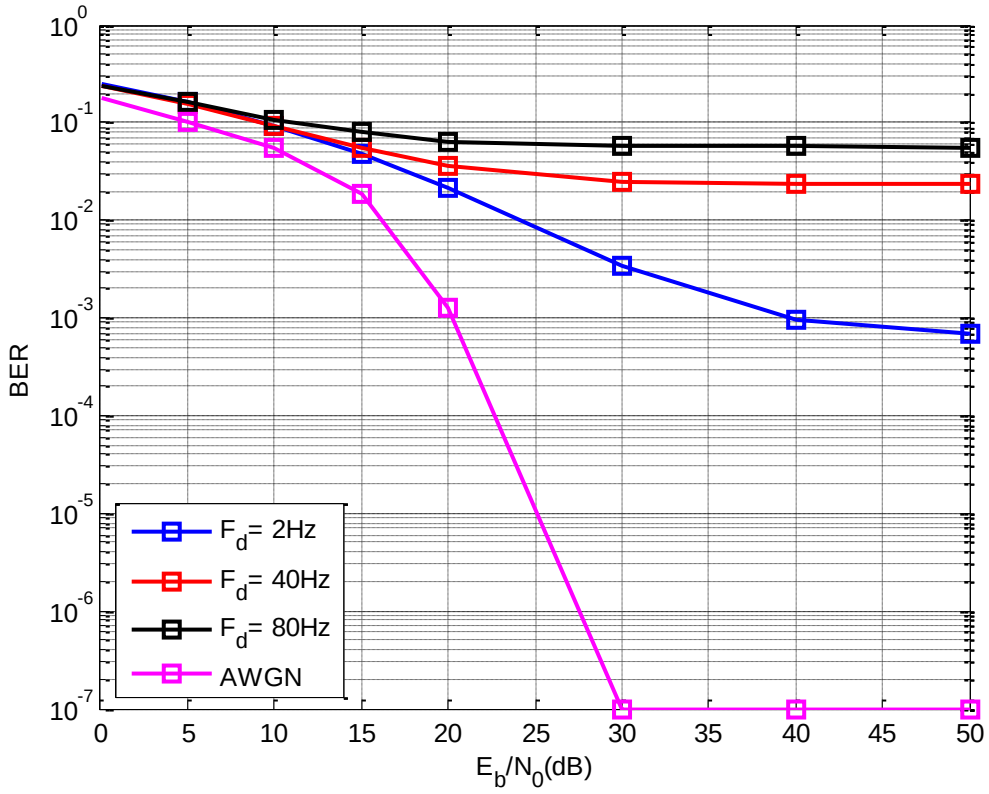

Figure 37. DVB-T system BERs over the CT8 channel for various noise and maximum Doppler shift levels.

LIST OF REFERENCES

[1] Y. Li, L. J. Cimini, Jr., and N. R. Sollenberger, "Robust channel estimation for OFDM systems with rapid dispersive fading channels," *IEEE Trans. Commun.*, vol. 46, no. 7, Jul. 1998.

[2] Y. Li, "Pilot-symbol-aided channel estimation for OFDM in wireless systems," *IEEE Trans. Vehicular Technology*, vol. 40, July 2000.

[3] H. Minn, D. I. Kim, and V. K. Bhargava, "A reduced complexity channel estimation for OFDM systems with transmit diversity in mobile wireless channels," *IEEE Trans. Commun.*, vol. 50, no. 5, May 2002.

[4] O. Edfors, M. Sandell, J.-J. van de Beek, S. K. Wilson, and P.O. Borjesson, "OFDM channel estimation by singular value decomposition," *IEEE Trans. Commun.*, vol. 46, no. 7, Jul. 1998.

[5] J. Wang, Z. Yang, C. Pan, J. Song, and L. Yang, "Iterative padding subtraction of the PN sequence for the TDS-OFDM over broadcast channels," *IEEE Trans. Consumer Electronics*, vol. 51, no. 4, pp. 1148–1152, 2005.

[6] B. Song, L. Gui, Y. Guan, and W. Zhang, "On channel estimation and equalization in TDS-OFDM based terrestrial HDTV broadcasting system," *IEEE Trans. Consumer Electronics*, vol. 51, no. 3, pp. 790–797, 2005.

[7] G. Liu and J. Zhang, "ITD-DFE based channel estimation and equalization in TDS-OFDM receivers," *IEEE Trans. Consum. Electron.*, vol. 53, no. 2, pp. 304–309, 2007.

[8] Y. Chen and Q. Liao, "Jointly channel estimation/equalization and subtraction of PN-ISI for TDS-OFDM systems over frequency-selective fading channels," *Int'l Conf. Commun. and Networking*, pp. 657–662, China, 2008.

[9] L. Gui, Q. Li, B. Liu, W. Zhang, and C. Zheng, "Low complexity channel estimation method for TDS-OFDM based Chinese DTTB system," *IEEE Trans. Consum. Electron.*, vol. 55, no. 3, pp. 1135–1140, 2009.

[10] B. Sklar. *The Characterization of Fading Channels*. [Online]. Available: http://faraday.ee.emu.edu.tr/ee569/art_sklar5_fading.pdf

[11] V. K. Grag, "Radio wave propagation," in *Wireless Communications and Networking*. San Francisco: Morgan Kaufmann, 2007, pp. 54–65.

[12] E. Biglieri, R. Gallager, and J. K. Wolf, "Channel models for digital transmission," in *Coding for Wireless Channels*. New York: Springer, 2005, pp. 21–24.

[13] D. Greene. (2013, Aug. 13). Modeling corruption. [Online]. Available: http://cnx.org/content/m46040/latest/#uid21

[14] Keysight Technologies. About fading. [Online]. Available: http://rfmw.em.keysight.com/wireless/helpfiles/n5106a/about_fading.htm

[15] M. Tummala, "Ad-hoc wireless networks," class notes for EC4745, Dept. of Electrical and Computer Engineering, Naval Postgraduate School, Apr. 2014.

[16] Rayleigh distribution. *Wikipedia*. [Online]. Available: http://en.wikipedia.org/wiki/File:Rayleigh_distributionPDF.svg

[17] HK Digital TV. An introduction to digital terrestrial television (DTT) broadcasting. [Online]. Available: http://www.digitaltv.gov.hk/consumer/pdf/DTT-PPT.pdf

[18] Digital terrestrial television. *Wikipedia*. [Online]. Available: http://en.wikipedia.org/wiki/Digital_terrestrial_television

[19] M. S. Richer, G. Reitmeier, T. Gurley, G. A. Jones, J. Whitaker, and R. Rast, "The ATSC digital television system," *Proc. of the IEEE, Special Issue on Global Digital Television: Technology and Emerging Services*, Jan. 2006, pp. 37–43.

[20] U. Ladebusch and C. A. Liss, "Terrestrial DVB (DVB-T): A broadcast technology for stationary portable and mobile use," *Proc. of the IEEE, Special Issue on Global Digital Television: Technology and Emerging Services*, Jan. 2006, pp. 183–194.

[21] M. Takada and M. Saito, "Transmission systems for ISDB-T," *Proc. of the IEEE, Special Issue on Global Digital Television: Technology and Emerging Services*, Jan. 2006, pp. 251–256.

[22] Surveys of Communication Standards by Students. "Wirelss LAN." [Online]. Dept. of Electrical, Computer, and Energy Engineering, Univ. of Colorado, Boulder. Available: http://ecee.colorado.edu/~ecen4242/wlana/wireless802.11a.html

[23] R. V. Nee and R. Prasad, *OFDM for Wireless Multimedia Communications*. Boston: Artech House, 2000.

[24] R. Cristi, "Digital signal processing for wireless communications," class notes for EC4910, Dept. of Electrical and Computer Engineering, Naval Postgraduate School, Summer 2013.

[25] Y.F. Jiang, "Implementation and validation of DVB-T transceiver in practical environments," M.S. thesis, Dept. Computer and Communication Engineering, National Taipei University of Technology, Taipei, Taiwan, 2011.

[26] Y. Xiao, "Orthogonal frequency multiplexing modulation and inter-carrier interference cancellation," M.S. thesis, Louisiana State University and Agricultural and Mechanical College, Baton Rouge, LA, 2003.

[27] H. Steendam and M. Moeneclaey, "Different guard interval techniques," in *Multi-Carrier Spread Spectrum 2007*. Germany: Springer Netherlands, 2007, pp. 11–24.

[28] R. Cristi, M. P. Fargues, and M. Hagstette "Detection of a week communication signal in the presence of a strong co-channel TV broadcast interferer," unpublished, Department of Electrical and Computer Engineering, Naval Postgraduate School, Oct. 2013.

[29] Office of the Telecommunications Authority (China). "Technical standard for digital terrestrial television broadcasting," Hong Kong, China, 2007.

[30] Ian Poole. What is DVB-T? [Online]. Available: http://www.radio-electronics.com/info/broadcast/digital-video-broadcasting/what-is-dvb-t-basics-31tutorial.php

[31] EBU.UER, "Digital video broadcasting (DVB): Framing structure, channel coding and modulation for digital terrestrial television," European Standard ETSI EN 300 744 v1.6.1, Sophia Antipolis Cedex, France, 2009.

[32] U. Ladebusch and C. A. Liss, "Terrestrial DVB (DVB-T): A broadcast technology for stationary portable and mobile use," in *Proc. of the IEEE*, vol. 94, no. 1, Jan. 2006, pp. 183–193.

[33] *Digital video broadcasting (DVB): Implementation guidelines for a second generation digital terrestrial television broadcasting system (DVB-T2)*, ETSI TS 102 831 v1.1.1 (2010-10).

[34] M. Liu, J. F. Hélard, and O. P. Pasquero, "Analysis and Performance Comparison of DVB-T and DTMB Systems for Terrestrial Digital TV," in *Proc. of the 11th IEEE Singapore Int. Conf. on Commun. Syst.* (*ICCS 2008*), Guangzhou, China, Nov. 2008, pp. 1399–1404.

[35] J. Wang, Z. X. Yang, C. Y. Pan, M. Han, and L. Yang, "A combined code acquisition and symbol timing recovery method for TDS-OFDM," *IEEE Trans. Broadcast.*, vol. 49, pp. 304–308, Sept. 2003.

[36] M. Liu, M. Crussiére, and J. F Hélard, "Improved channel estimation methods based on PN sequence for TDS-OFDM," *IEEE Trans. Broadcast.*, vol. 56, no. 3, pp. 418–424, 2010.

[37] I.C. Liu et al., "Modified DFT-Based Channel Estimation for TDS-OFDM Communication Systems," in *ISPACS Symp.*, Naha, pp. 108–113, Nov. 2013.

[38] COST 207 Management Committee, *COST 207: Digital Land Mobile Radio Communications, Final Report*, Commission of the European Communities, 1989.

[39] M. Failli, "Digital land mobile radio communications," *CIC Inf. Technol. and Sci.*, Brussels, Belgium, COST 207 Final Rep., 1989, pp. 135–166.

[40] R. Cristi, private communication, Sep. 2013.

INITIAL DISTRIBUTION LIST

1. Defense Technical Information Center
   Ft. Belvoir, Virginia

2. Dudley Knox Library
   Naval Postgraduate School
   Monterey, California